Lithos 320–321 (2018) 315–331

Contents lists available at ScienceDirect

Lithos

journal homepage: www.elsevier.com/locate/lithos

U-Pb Geochronology and Geochemistry of the Povungnituk Group of the Cape Smith Belt: Part of a Craton-Scale Circa 2.0 Ga Minto-Povungnituk Large Igneous Province, Northern Superior Craton

N. Kastek [a,b,*], R.E. Ernst [a,b], B.L. Cousens [a,b], S.L. Kamo [c], W. Bleeker [d], U. Söderlund [e], W.R.A. Baragar [d], P. Sylvester [f]

[a] Department of Earth Sciences, Carleton University, 1125 Colonel By Drive, Ottawa, ON K1S 5B6, Canada
[b] Faculty of Geology and Geography, Tomsk State University, 36 Lenin Ave, Tomsk 634050, Russia
[c] University of Toronto, 22 Russell Street, Toronto, ON M5S 3B1, Canada
[d] Geological Survey of Canada, Ottawa, ON K1A 0E8, Canada
[e] Department of Earth & Ecosystem Sciences, Lund U,Sweden
[f] Texas Tech University, 125 Science Building, Lubbock, TX79409-1053, USA

ARTICLE INFO

Article history:
Received 28 June 2018
Accepted 23 September 2018
Available online 27 September 2018

Keywords:
Cape Smith belt
Superior craton
Large igenous province
Mantle plume
Povungnituk flood basalts
Minto dykes

ABSTRACT

Magmatism of the Povungnituk Group of the Cape Smith Belt, northern Superior craton, was formed in three stages: (i)early alkaline magmatism and associated carbonatites (undated), (ii) a main flood basalt sequence (Beauparlant Formation) (constrained between 2040 and 1991 Ma), and (iii) a late stage alkaline pulse (Cecilia Formation) (ca. 1959 Ma). We suggest that the main stage of magmatic activity (middle pulse) was of short duration.

A new U—Pb baddeleyite age of 1998 ± 6 Ma is obtained from a dolerite sill intruding the uppermost section of the Beauparlant Formation. This age has regional significance because it matches the previously obtained 1998 ± 2 Ma age for the Watts Group (Purtuniq) ophiolite of the northern Cape Smith Belt and the 1998 ± 2 Ma U-Pb age of the Minto dykes intruding the craton to the south. These coeval units, along with additional units correlated on paleomagnetic grounds (Eskimo Formation), are interpreted to define a large igneous province (LIP), extending over an area of >400,000 km^2, which we herein define as the Minto-Povungnituk LIP.

Geochemical comparison between the Watts Group ophiolite, Minto dykes and the mafic Povungnituk Group shows significant differences allowing these data to be divided into two groups and domains within the LIP. A northern domain, comprising the Povungnituk and Watts groups, shows mixing between a depleted mantle source and a more enriched mantle plume-sourced melt. A southern domain comprising the Minto dykes and the paleomagnetically linked Eskimo Formation shows signs of an even more enriched source, while these magmas also show the effect of crustal contamination.

Two distinct source mechanisms can be responsible for the observed geochemical differences between the two domains. First, a difference in lithospheric sources, where melting of different portions of Superior craton lithosphere caused the different melt signatures in the interior of the craton. In this case magmatism in the two domains is only related by having the same heat source (e.g.,a mantle plume) interpreted to be located on the northwestern side of the northern Superior craton. Second, two distinct deep mantle sources that remained separated within the ascending plume. This is analogous to some current hotspots interpreted to sample both large low shear velocity provinces (LLSVP) and adjacent ambient deep mantle. This latter interpretation would allow for the use of bilateral chemistry in LIPs as a potential tool for the recognition and mapping of the LLSVP boundaries throughout Earth's history.

1. Introduction

Large igneous provinces (LIPs) have become an important focus for research in recent years due to their use in paleocontinental reconstructions (e.g.,Bleeker and Ernst, 2006; Ernst et al., 2013), in exploration targeting (e.g., Ernst and Jowitt, 2013, 2017), and as a result of their

* Corresponding author at: Department of Earth Sciences, Carleton University, 1125 Colonel By Drive, Ottawa, ON K1S 5B6, Canada.
E-mail address: nico.kastek@carleton.ca (N. Kastek).

https://doi.org/10.1016/j.lithos.2018.09.026
0024-4937/

links to dramatic climate change (e.g., Ernst and Youbi, 2017; Wignall, 2001, 2005). LIPs represent large volume (>0.1 Mkm^3; frequently above 1 Mkm^3), mainly mafic (−ultramafic) magmatic events of intraplate affinity (based on tectonic setting and/or geochemistry) that occur in both continental and oceanic settings, and are typically either of short duration (<5 Ma) or consist of multiple short pulses over a maximum of a few 10s of Myr. LIPs comprise volcanic packages (flood basalts) and a plumbing system of dyke swarms, sill complexes, layered intrusions, and a magmatic underplate (Bryan and Ernst, 2008; Coffin and Eldholm, 1991, 1992; Ernst, 2014).

Numerous diabase dyke swarms and associated magmatism, mostly of Proterozoic age, intrude the Superior craton, and are thought to record periodic LIP magmatism (e.g., Ernst and Bleeker, 2010). One of the more dramatic LIP remnants occurs in the Cape Smith Belt in the northernmost part of the Quebec promontory of the Superior craton. The Cape Smith Belt is dominated by the Povungnituk basalts (Franics et al., 1983; Hynes and Francis, 1982), interpreted as continental flood basalts, and associated dolerite sills which are broadly constrained in age between 2.04 and 1.91 Ga (Machado et al., 1993), and the younger ca. 1882 Ma Chukotat event (Bleeker and Kamo, 2018; Randall, 2005; Wodicka et al., 2002) (Fig. 1).

This research provides a precise age and new geochemical data for the Povungnituk Group, links it with additional coeval units into a regional LIP, and then integrates the chemistry of all the units in order to develop a petrogenetic and geodynamic model for the emplacement of the LIP.

2. Geological setting

The Cape Smith fold and thrust belt (Fig. 1) is located at the northern tip of Quebec, composed of a fold thrust-belt of the Paleoproterozoic Ungava orogen (Bleeker and Kamo, 2018; St-Onge et al., 1992). It contains well-preservedvolcano-sedimentary and plutonic suites, which overlie Archean tonalites and gneisses of the northern Superior craton. The Cape Smith fold and thrust belt can be subdivided into a northern allochthonous, and a southern allochthonous to parautochthonous domain. These two domains had contrasting metamorphic and tectonic histories, until they were amalgamated, further deformed, and imbricated during the during terminal collision of the Superior craton with the Archean and Rae cratons to the north and the climax of the Trans-Hudson Orogeny at ca. 1838 Ma (Corrigan, 2012; St-Onge et al., 2006). The northern domain contains crustal components, interpreted as an c. 1998 Ma ophiolite complex (Watts Group) (Scott et al., 1999) and a c. 1860 Ma forearc complex (Parent Group, Spartan Group) (St-Onge et al., 1992). The southern domain comprises the c. 2040–1960 Ma Povungnituk and c. 1880 Ma Chukotat Groups.

At its base the Povungnituk Group consists of the Dumas Formation (also referred to as the Lamarche Group), which represents an autochthonous to parautochthonous assemblage of ferruginous sandstone, conglomerate, quartzite and iron formation, overlain by progressively finer-grained wackes and rare carbonates. It unconformably overlies the Superior craton basement. These rocks represent continent-derived sediments accumulated in a continental rift basin environment (St-Onge et al., 1992).

The Dumas Formation is overlain by the predominantly basaltic Beauparlant Formation which in turn is overlain by the sedimentary Nuvilik Formation. The Beauparlant Formation comprises tholeiitic basalts that occur both as pillowed and tabular basalt flows intercalated with volcanoclastic and locally graphitic siltstone horizons and minor carbonate sedimentary rocks. Geochemical constraints on the Povungnituk volcanism have been developed in previous studies and are discussed in Section7.1 (Dunphy et al., 1995; Franics et al., 1983; Hegner and Bevier, 1991; Hynes and Francis, 1982; Legault et al., 1994; Modeland et al., 2003; Picard, 1989a; Picard, 1989b).

A mafic sill in the upper Dumas Formation is 2038 ± 3 Ma (Machado et al., 1993) and was originally considered to be comagmatic with volcanic rocks of the Beauparlant Formation (see alternative interpretation below). At a higher stratigraphic level, a small granodiorite intrusion in Povungnituk pillow basalts has a robust zircon age of 1991 ± 2 Ma (Machado et al., 1993). Therefore, the main part of the Beauparlant Formation must predate 1991 Ma. These age constraints show that Povungnituk magmatism occurred between 2038 and 1991 Ma.

The majority of Povungnituk magmatism occurred, therefore, in the timespan from 2040 Ma and 1991 Ma. However, it is important to obtain better constraints on the age of this flood basalt event, and preferably a direct age on the mafic magmatism to properly identify units belonging to this event and also units on other blocks that can be correlated in a paleocontinental reconstruction.

Although tholeiitic basalts dominate the Povungnituk Group, small alkaline volcanic suites have also been documented. Near the base of the succession, in the western portion of the Cape Smith fold belt, occur carbonate-rich alkaline lavas as described by Baragar et al. (2001). This Lac Leclair volcanic suite comprises a 500 m-thick sequence of carbonatitic, ultramafic lapilli tuffs and lavas that outcrop along the southern extremity of the belt, near the unconformity with the Superior craton. The presence of the Lac Leclair volcanic suite among the

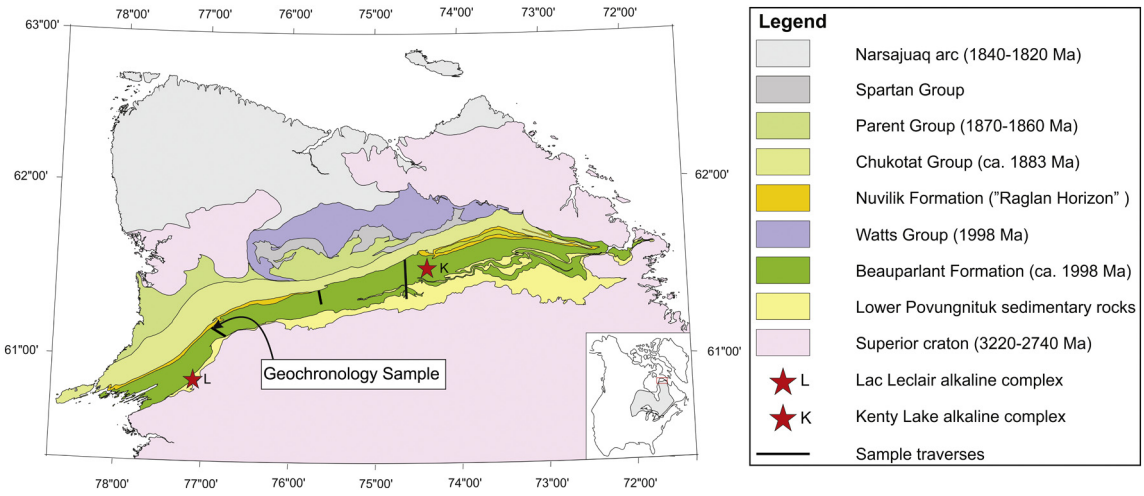

Fig. 1. Geological map of the Ungava Orogen, northern Quebec, Canada (after St-Onge et al., 2004). Stars represent the location of the Lac Leclair alkaline complex from Baragar et al. (2001) and the Kenty Lake alkaline complex from Gaonac'h et al. (1992). Traverses are from Baragar (2015, 2017)

platformal sedimentary rocks of the lowermost Povungnituk Group indicates that it may be one of the first volcanic manifestations of rifting and subsidence during the development of the Cape Smith fold belt (Baragar et al., 2001).

Another alkaline volcanic package is exposed in two adjacent thrust blocks near the top of the Beauparlant Formation in the Cecilia and Kenty Lake areas (Gaonac'h et al., 1992). This alkaline suite is several hundred meters thick, and comprises a lower sequence of basanites and nephelinites intercalated with pyroclastic deposits and an upper sequence of trachytic lavas with rare alkali-feldspar phenocrysts (Gaonac'h et al., 1992). A rhyolite sample from this suite has been dated at 1958 ± 3 Ma (Parrish, 1989). This age marks a late-stage magmatic pulse and constrains the overlying sedimentary Nuvilik Formation to be younger than 1959 Ma.

The Beauparlant Formation is overlain by a succession of deep-water sedimentary rocks of the Nuvilik Formation, including greywackes, cherts, and graphitic argillites and rare pebbly quartz arenites (Mungall, 2007). In some parts of the Cape Smith Belt, the Nuvilik Formation overlies alkaline volcanic rocks of the Cecilia Formation (Picard, 1995).Based on a re-evaluation of the Povungnituk stratigraphy (Bleeker and Kamo, 2018) it was concluded that the contact between the uppermost pillow basalt of the Beauparlant Formation and the base of the Nuvilik Formation is conformable. Furthermore, there is no evidence for a thrust fault at the top of the Nuvilik Formation, and therefore the Nuvilik Formation does not represent a tectonically transported metasedimentary package equivalent to the Dumas Formation, as was previously proposed by Lucas and St-Onge (1992) (cf. Bleeker and Ames, 2017 for discussion). The depositional age and detrital source of the Nuvilik Formation is not known. Its time of deposition may span the interval from ca. 1959 Ma to ca. 1883 Ma (as discussed below).

The Nuvilik Formation is overlain by the accumulation of the ca. 1882–1874 Ma predominantly volcanic deep-water assemblage of the Chukotat Group (Francis and Hynes, 1979; Franics et al., 1983; Hynes and Francis, 1982).

The Chukotat Group comprises a succession of mafic volcanic rocks that records a transition in chemical composition from rift-related (Povungnituk Group) to mid-ocean ridge basalt (MORB)-like (Chukotat Group) composition (Francis et al., 1981; Franics et al., 1983; Picard, 1989a; Picard, 1989b; St-Onge et al., 1992) and is part of the Circum Superior LIP (e.g. Ciborowski et al., 2017; Ernst, 2014; Heaman et al., 2009; Minifie et al., 2013).

The strata of the Povungnituk Group were intruded at 1882.7 ± 1.3 Ma (Randall, 2005) by a series of mafic to ultramafic bodies of the Expo Intrusive Suite (Mungall, 2007). The Expo Intrusive Suite, the Raglan Formation and the Chukotat Group can be considered a single magmatic suite, based on age similarity and the match between the observed and proposed primitive magmas (Mungall, 2007).

The volcanics of the Povungnituk Group of the Cape Smith Belt, in particular in the western part, has been linked to various other magmatic units in the Superior craton to the south based on geochronological and geochemical evidence (Buchan et al., 1998, 2007; Legault et al., 1994; Parrish, 1989; Schmidt, 1980; Schwarz and Fujiwara, 1981). These include the Minto dykes, Eskimo volcanics, Nastapoka basalts and Persillon volcanic rocks in the Richmond Gulf area, and Inukjuak dykes Halls and Davis (2004) viewed these units as the product of a 2.0 Ga rifting event, located beneath modern day Hudson Bay, that caused a relative rotation of the eastern and western Superior craton. The magmatic event associated with that rifting may corresponds to what we are describing herein as the Minto-PovungnitukLIP, which includes the Minto and Inukjuak dyke swarms east of Hudson Bay, Eskimo volcanics of the Belcher Islands, Nastapoka basalts and Persillon volcanic rocks of the Richmond Gulf, Povungnituk volcanics and the Watts Group of the Cape Smith Belt. Scott et al. (1999) and Hamilton et al. (2016) have suggested a mantle plume as the context for this 2 Ga magmatism. Geochemistry will also help assess whether a mantle plume was involved and whether the magmatism is associated with thinned lithosphere (which could also support the role of rifting), and to identify any spatial variations in chemistry that can be related to different mantle sources.

To provide this geochemistry assessment, we have reanalyzed material previously collected from the Povungnituk Group. We have utilized high quality geochemistry data from the literature for the Watts Group, Minto dykes, and Eskimo Formation and have obtained Nd isotopes for the Minto dykes that have not been available before.

3. Sample selection

Samples for geochemistry and petrography from the mafic Povungnituk Group (MPG) were collected by W.R.A. Baragar during a 1973 field season with the Geological Survey of Canada. Petrography and major element chemistry of three traverses (Figs. 1, 2) were published in Baragar (2015, 2017). The samples were collected over three transects through the MPG, spanning an inferred volcanic thickness of 3 km; although fault duplication has been proposed (St-Onge et al., 1992), it has been considered unlikely by Mungall (2007) and Bleeker and Ames (2017) (see discussion in Section6.1.2). Baragar's 84 samples (reanalyzed in our study) were collected in chips over a distance of roughly one meter in homogenous units for each geochemistry sample and as selected large hand samples for geochronology. In order to address the above research objectives, new Nd isotopes and a new U—Pb age were produced for a selected suite of the MPG.

In addition, geochemical data for seven samples from four WNW-NW trending Minto dykes were included. These data were from Ernst and Buchan (2010), who analyzed samples from Buchan et al. (1998). These Minto dyke samples were then further analyzed for Nd-isotopes as part of this research (see below).

Several samples were processed for U—Pb dating but only one sample yielded baddeleyite. This dated sample (BLS-73-31) is from the lower part of a dolerite sill at the very top of exposed western Povungnituk Group rocks. It is separated from the Chukotat lavas to the north by a highly contorted shale unit that presumably marks the presence of a thrust fault somewhere in close proximity.

4. Methodology

4.1. U—Pb geochronology

Baddeleyite was separated from dolerite sample BLS-73-31 at both the Lund University and University of Toronto laboratories. U—Pb ID-TIMS dating was carried out in Toronto.

At the Lund University laboratory, ~500 g of sample was crushed into cm-size pieces using a sledgehammer and placed in a mill tray to produce a fine powder. The suspended sample was put in portions consisting of ~20–40 g on a Wilfley water-shaking table following the procedures in Söderlund and Johansson (2002). After 2–3 cycles in which suspended powder was loaded onto the shaking table and the lighter material washed away, the remaining heavier fraction was then transferred into a small glass petri dish. The magnetic minerals were removed using a pencil magnet. Baddeleyite grains were hand-picked under a binocular microscope and the best quality grains were selected for isotopic analysis. The selected baddeleyite grains were dark brown, crystalline, and with no trace of alteration (i.e.,no visible frosty zircon rims).

Additional baddeleyites were also separated from this sample at the Jack Satterly Geochronology laboratory of the University of Toronto using a similar procedure to that of Lund University (see above). The mineral fractions chosen for analysis comprised between 2 and 7 grains of baddeleyite.

At the University of Toronto laboratory, selected baddeleyite crystals were given a brief wash in HNO_3, spiked using a mixed ^{205}Pb—^{235}U isotopic tracer, and dissolved in a 12:1 volume of

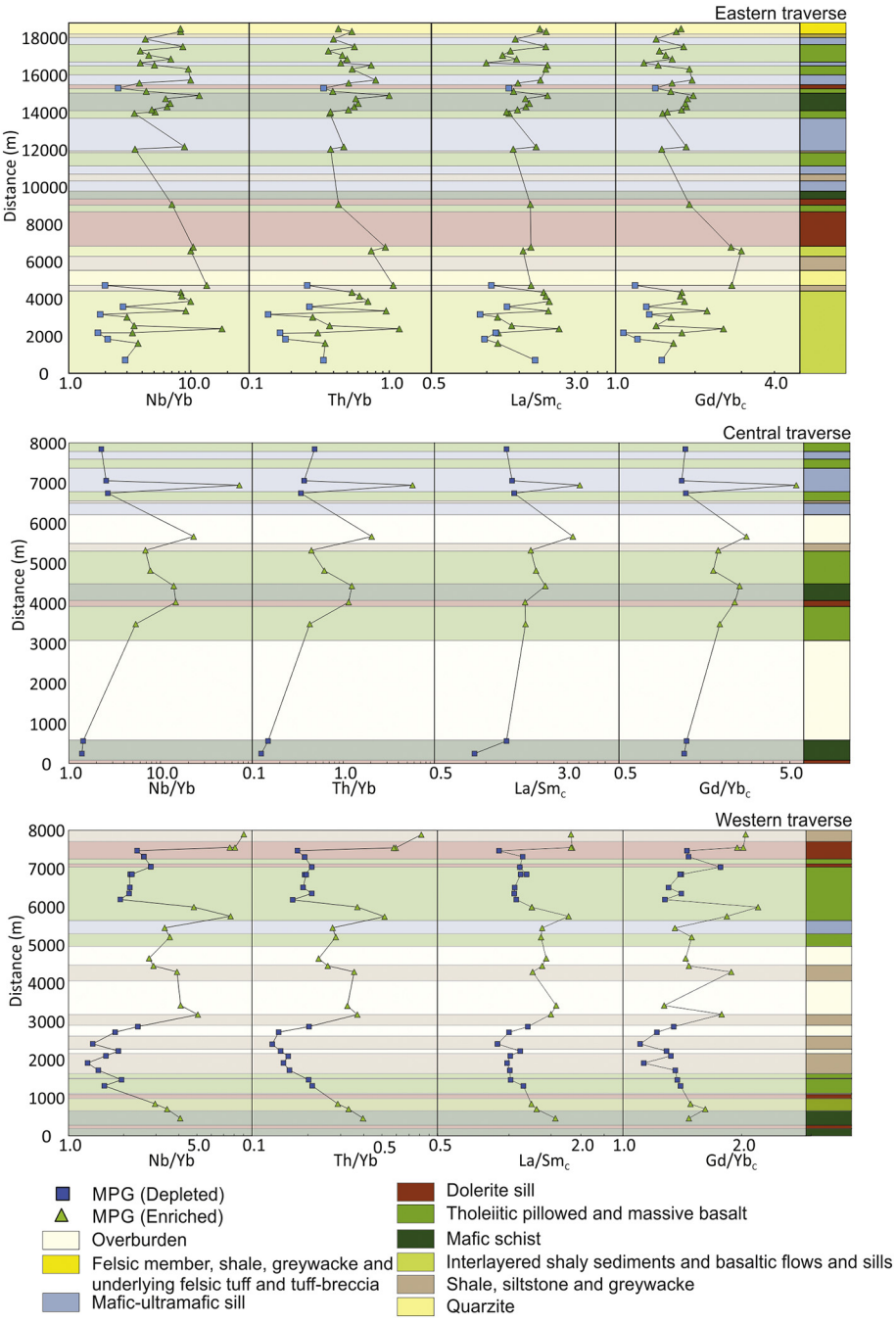

Fig. 2. Selected element ratios along the traverses shown in Fig. 1 from East (top) to West (bottom). Stratigraphic columns modified from Baragar (2015) and Baragar (2017). Rare earth elements normalized to chrondrite. Values from Sun and McDonough (1989).

HF-HNO_3 acid in Teflon® bombs at 200 °C (Krogh, 1973a,b). Samples were redissolved in 3 N HCl in preparation for anion exchange chemistry, dried down with dilute phosphoric acid and loaded with silica gel onto zone-refined rhenium filaments. Isotopic compositions of Pb and U were determined on a M354 mass spectrometer using a Daly detector in digital pulse-counting mode. A Daly mass fractionation correction of 0.05% per atomic mass unit (AMU), and a thermal mass discrimination correction of 0.1% per AMU for Pb and U, was applied. Dead-time of the counting system during the analytical interval was 16 ns based on measurements of the NBS SRM 982 Pb standard. Laboratory procedural blanks at the Jack Satterly Geochronology Laboratory are routinely at the 0.5 pg and 0.1 pg level or less for Pb and U, respectively.

4.2. Geochemistry

4.2.1. Major and trace element analyses

All 84 sample powders from the Povungnituk suite, including an internal standard (10–LT–05, a basaltic andesite from Lake Tahoe, California) were sent to ALS Geochemistry laboratories in North Vancouver, British Columbia for major element analysis via Inductively Coupled Plasma Atomic Emissions Spectrometry (ICP–AES) as well as trace and rare earth element (REE) analysis via Inductively Coupled Plasma Mass Spectrometry (ICP-MS). Major- and trace-element analytical uncertainties (2σ) for ALS Geochemistry laboratories based on repeat analysis of the Lake Tahoe internal standard are reported in the Supplementary Data.

4.2.2. Sm—Nd isotopes analysis

Rock powders were spiked with a mixed ^{148}Nd—^{149}Sm spike before being dissolved in a mixed solution of ~29 M HF and ~16 M HNO_3. The samples were then dried down on a hotplate before being redissolved with 8 M HNO_3 and 6 M HCl sequentially. The dried residue of each sample was finally dissolved in 2.5 M HCl prior to being loaded onto 14 ml Bio-Rad borosilicate glass chromatography columns containing 3.0 ml of Dowex AG50W–X8 cation resin. REE were eluted with 6 M HCl. REE fractions were then dissolved in 0.26 M HCl and loaded onto Eichrom Ln Resin chromatographic columns containing Teflon powder coated with HDEHP [di(2-ethylhexyl) orthophosphoric acid] (Richard et al., 1976). Nd was eluted with 0.26 M HCl, followed by Sm with 0.5 M HCl. The isotope ratios were measured using a Thermo Finnigan Triton thermal ionization mass spectrometer (TIMS) housed at the Isotope Geochemistry and Geochronology Research Centre (IGGRC), Carleton University, Ottawa, Canada. Nd and Sm fractions were loaded with H_3PO_4 onto one side of a double rhenium filament assembly. The isotope ratios were measured at temperatures of 1700–1800 °C and are normalized to $^{146}Nd/^{144}Nd = 0.72190$. An IGGRC's in-house Nd standard was routinely measured and an average value of the $^{143}Nd/^{144}Nd$ ratio was 0.511826 ± 0.000007 (1σ) over a period of three years; this value is equivalent to $^{143}Nd/^{144}Nd = 0.511855$ reported for the La Jolla Nd standard. Sm and Nd concentrations were measured precisely within 1%, whereas $^{147}Sm/^{144}Nd$ ratios are reproducible to 0.5%. Analyses of the USGS standard BCR-2 yield Nd = 28.53 ppm, Sm = 6.618 ppm, and $^{143}Nd/^{144}Nd = 0.512643 \pm 0.000011$ ($n = 13$, 2σ). Total procedural blanks for Nd are <50 picograms.

5. Results

5.1. Field Observations

The MPG consists of mainly massive, basaltic flows with rare pillows and sills interlayered with black shale and greywacke, tuff, pyroclastic rocks and, in places, siliceous material (Mungall, 2007; St-Onge et al., 1992). Northward (up section), the MPG is increasingly dominated by pillowed and massive tholeiitic basalt with minor interflow black shale, cherty sediment, tuff and agglomeritic tuff (Fig. 2). This study focuses on the basalts and associated dolerites.

The general petrography of the three traverses across the Cape Smith Belt are summarized here. Both volcanic rocks and dolerites are present, the latter probably reflecting associated sills or thick flows. The dolerite samples commonly preserve a vestige of igneous texture mainly in the distribution of the mafic minerals and feldspar, and most samples have little or no foliation. All doleritic rocks are at greenschist facies and the mineralogy is typical of this low metamorphic grade. Sodic plagioclase is intergrown with actinolite and chlorite, in roughly equal proportions, epidote is subordinate, and titanite, commonly enclosing relics of opaque minerals, is accessory. Sparsely distributed blebs of chlorite observed in some dolerite sills are interpreted as pseudomorphs after olivine. The volcanic rocks are of similar mineralogy, but finer grained, and are commonly sparsely plagioclase phyric. They generally show some degree of foliation development.

5.2. U—Pb geochronology

Results of U—Pb ID-TIMS analysis of five fractions of baddeleyite (B1 to B5) from dolerite sill sample BLS-73-31 are summarized in Table 1 and plotted in Fig. 3. The U—Pb data are variably discordant and define a Pb loss array (red ellipses in Fig. 3) that intersects the concordia curve at 2004 ± 24 Ma and 1303 ± 410 Ma, with an MSWD of 2.0. Fraction B3 plots slightly below the linear array and if omitted from the regression line calculation results in reduced scatter (MSWD = 0.17), and upper and lower intercept ages of 1998 ± 20 Ma and 1251 ± 420 Ma.

The baddeleyite grains were apparently affected by variable degrees of ancient Pb loss (for example, from Raglan events ca. 1881–1882 Ma and younger metamorphism), perhaps in addition to minor later Pb loss during final uplift and exposure. The apparent lower intercepts likely result from time-averaged Pb loss and are not considered geologically significant. Anchoring the Pb loss line at ca. 1250 Ma does not affect the calculated age, and yields 1998 ± 6 Ma (Fig. 3), which is interpreted to represent a maximum age for the emplacement of the dolerite sill.

A line through fractions B1 and B3 defines a steeper Pb loss line to an upper intercept of 1988 ± 10 Ma, which can be interpreted as a minimum age estimate for the dolerite. As fractions B1 and B3 are less discordant and less affected by earlier open system behaviour (in contrast to fractions B4 and B5), the corresponding Pb loss line may provide a more accurate upper intercept age (e.g., Bleeker, 2014). The $^{207}Pb/^{206}Pb$ age of least discordant fraction B1, at 1986 ± 5 Ma, defines an absolute minimum age.

An age interpretation of 1998 ± 6 Ma, or one intermediate between 1988 Ma and 1998 Ma (based on the above discussion), is in agreement with the earlier age determination for Povungnituk Group magmatism of 1991 ± 2 Ma (Machado et al., 1993), and also overlaps with the age determined for one of the Minto dykes (Buchan et al., 1998). This dated sample is interpreted (by W.R.A. Baragar) as a sill or coarse-grained flow. If it is a sill, then strictly speaking this U—Pb date is a

Table 1
U—Pb isotopic results for baddeleyite crystals from a dolerite sill that intrudes the Beauparlant Formation, Povungnituk Group, Cape Smith Belt, Quebec.

No.	U (ppm)	Th/U	Pb_T (pg)	Pb_C (pg)	$^{206}Pb/^{204}Pb$ measured	$^{207}Pb/^{235}U$	2 σ	$^{206}Pb/^{238}U$	2 σ	Error Corr	$^{207}Pb/^{206}Pb$	2 σ	$^{206}Pb/^{238}U$ Age (Ma)	2 σ	$^{207}Pb/^{235}U$ Age (Ma)	2 σ	$^{207}Pb/^{206}Pb$ Age (Ma)	2 σ	% Disc
BLS 31 73																			
B1	1767	0.16	19.0	0.6	2222	6.020	0.025	0.3579	0.0011	0.794	0.1220	0.0003	1972	5	1979	4	1986	5	0.8
B2	720	0.25	15.7	0.3	2992	5.933	0.024	0.3546	0.0011	0.839	0.1213	0.0003	1957	5	1966	3	1976	4	1.1
B3	160	0.20	11.3	0.2	3651	5.944	0.027	0.3540	0.0015	0.921	0.1218	0.0002	1954	7	1968	4	1982	3	1.7
B4	582	0.48	17.8	0.6	1777	5.883	0.027	0.3524	0.0012	0.792	0.1211	0.0003	1946	6	1959	4	1972	5	1.5
B5	416	0.23	11.8	1.4	551	5.800	0.078	0.3489	0.0019	0.651	0.1206	0.0013	1929	9	1946	12	1965	19	2.1

Notes:
Th/U calculated from radiogenic $^{208}Pb/^{206}Pb$ ratio and $^{207}Pb/^{206}Pb$ age assuming concordance.
Pb_T is total amount of Pb excluding blank.
Pb_C is total amount of common Pb in picograms; assigned the isotopic composition of laboratory blank.
$^{206}Pb/^{204}Pb$ corrected for fractionation and common Pb in the spike.
Pb/U ratios corrected for fractionation, common Pb in the spike, and blank.
Correction for ^{230}Th disequilibrium in $^{206}Pb/^{238}U$ and $^{207}Pb/^{206}Pb$ assuming Th/U of 4.2 in the magma.
Error Corr is correlation coefficients of X-Y errors on the concordia plot.
Disc is percent discordance for the given $^{207}Pb/^{206}Pb$ age.
Baddeleyite fractions B1, B2, B3, B4 and B5 consisted of, respectively, one larger and one small dark brown grain, four medium-sized brown blades, three laths, seven small brown blades, two larger blades.

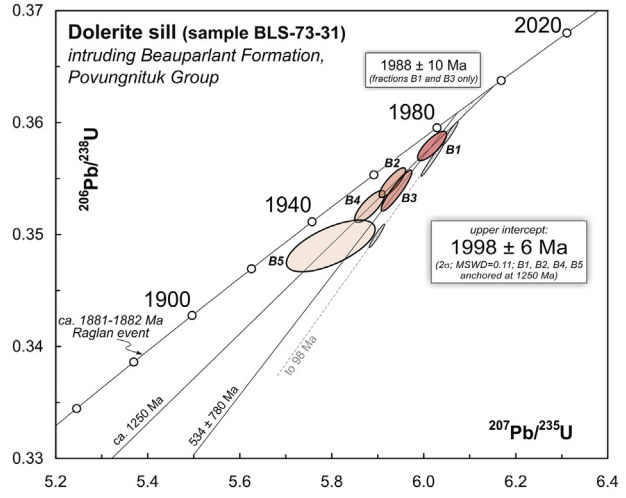

Fig. 3. U—Pb concordia diagram for dolerite sample BLS-73-31 within the Povungnituk Group volcanic sequence, showing results for five non-abraded baddeleyite fractions (red ellipses, B1 to B5). The results are variably discordant along a Pb loss line (B1 is least discordant at 0.8% from its $^{207}Pb/^{206}Pb$ age of 1985 Ma). The upper intercept through four data, at 1998 ± 6 Ma, represents a reasonable age interpretation, although the true crystallization age may be slightly younger, intermediate between 1998 ± 6 Ma and 1988 ± 10 Ma, a minimum age estimate based on B1 and B3. The age is in agreement with zircon data (grey ellipses, shown for reference) on a small granodiorite intrusion in pillow basalts of the Povungnituk Goup (Machado et al., 1993).

minimum age for the age of the flood basalts. However, the geochemistry of this sill (and of other similar sills/coarse-grained flows) matches the chemistry of the flows (Fig. 4), and therefore confirms this U—Pb age as representing an age for the flood basalts (specifically the enriched magma type).

5.3. Major and trace elements

The results for major and trace elements are shown for representative samples in Table 2. Element mobility during metamorphism needs to be considered for the MPG. The entire belt has undergone greenschist to lower amphibolite facies metamorphism (St-Onge et al., 1992) and the rocks commonly have LOI >2 wt%. Most element concentrations therefore need to be viewed with caution. Other relatively immobile elements such as the high field-strength elements (e.g., Nb and Zr) and REE (e.g., La and Sm), particularly their ratios, have been shown to be relatively immobile and thus are believed to preserve a record of the magmatic processes (e.g. Pearce, 2008). In comparison with these immobile elements, some major and trace elements in the MPG display varying degrees of scatter and have been avoided for geochemistry in this study. These include Si, Ca, K, Na, Rb, Sr, Cs, Ba and U.

The chemical compositions of the MPG lavas are quartz-normative, Fe and Ti-rich basalts. Their relatively evolved nature is indicated by their low MgO contents (range ~6 wt%, with maximum of ~10 wt%) and elevated Fe_2O_3 contents (range ~17 wt%). Al_2O_3 content is positively correlated with Mg# (Fig. 4a). Zirconium and Sc concentrations are negatively correlated with Mg# (Fig. 4c, d). On the basis of Zr/Ti vs. Nb/Y systematics (Pearce and Norry, 1979) the MPG varies in composition from basalt to alkaline basalt (Fig. 5a). Rare earth element diagrams display a large variation of trends, with samples showing MORB-like La/Yb_C trends (La/Yb_C between 1 and 2)and fanning towards OIB-like trends (La/Yb_C between 2 and 10) (Fig. 5b). This is supported by primitive mantle normalized incompatible trace element patterns, where MPG samples vary between *E*-MORB and OIB as characterized by Sun and McDonough (1989)(Fig. 5c). In a Th/Yb vs. Nb/Yb plot (Pearce, 2008) (Fig. 5d), all MPG samples fall along the mantle array, forming a trend between E-MORB and OIB end member compositions. The absence of elevated Th/Yb ratios (Fig. 5d) indicates no or only minor interaction with crustal material. Th/Nb_{PM} ratios are also a good monitor of crustal input (e.g., Wang et al., 2002) and Th/Nb_{PM} data for MPG sample (not shown) also show no correlation with Mg# and form a cloud between 0.6 and 1. Thus, based on major and trace element behaviour two compositional end members have therefore been involved in the formation of the MPG and can be identified as a depleted E-MORB-like group and a more enriched OIB-like group.

As shown in Figs. 4 and 5, samples that can be clearly defined as sills overlap geochemically with the samples that can be clearly identified in the field as flows, as well as with the samples for which no clear emplacement method can be determined. This overlap occurs in the

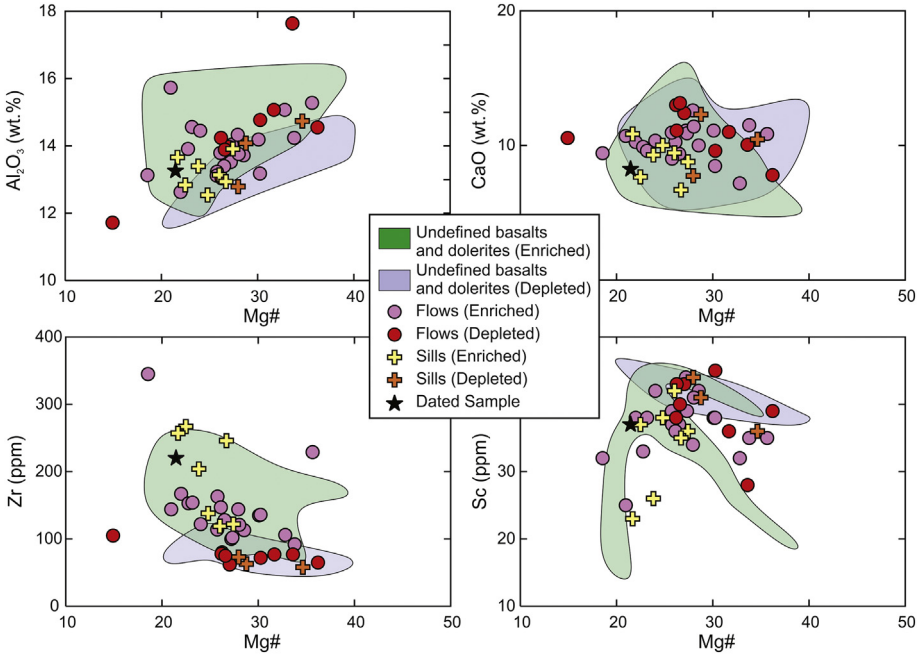

Fig. 4. Selected elements for the mafic Povungnituk Group (MPG) versus Mg-number (Mg#: molar MgO/(MgO + FeO*100).

Table 2
Representative geochemical data from the Mafic Povungnituk group.

Sample	BLS 57 73	BLS 55 73	BLS 34 73	BLS 53 73	BLS 183 73	BLS 31 73	BLS 264 73	BLS 182 73
Location	K1-28A	K1-30	K1-07	K1-32	C1-41	K1-04	N4-02	C1-40
Traverse	West	West	West	West	Central	West	East	Central
Group	Depleted	Depleted	Depleted	Enriched	Enriched	Enriched	Enriched	Enriched
Easting	401,889	402,205	396,393	402,874	462,536	395,889	519,628	462,608
Northing	6,779,706	6,779,411	6,781,526	6,779,219	6,801,174	6,781,752	6,815,745	6,801,726
SiO2	47.40	48.50	48.00	46.60	46.40	44.80	43.00	40.50
Al2O3	13.50	13.10	13.30	12.50	13.95	12.85	14.25	14.40
Fe2O3	13.45	14.85	14.65	15.70	13.30	16.85	16.75	13.60
CaO	12.30	10.45	10.50	10.05	9.01	8.23	8.46	8.51
MgO	6.30	6.50	7.02	6.21	8.06	5.34	6.82	3.69
Na2O	1.23	2.56	2.44	2.34	2.99	2.83	2.41	4.76
K2O	0.02	0.14	0.12	0.23	0.17	0.57	0.61	0.53
TiO2	1.03	1.37	1.52	1.77	1.84	3.03	3.63	3.07
MnO	0.22	0.21	0.20	0.23	0.25	0.24	0.27	0.34
P2O5	0.07	0.12	0.11	0.16	0.12	0.37	0.57	0.42
LOI	4.12	2.06	2.84	2.38	2.94	3.01	2.93	8.31
Total	99.68	99.9	100.76	98.24	99.12	98.18	99.78	98.18
Mg#	29	27	29	25	34	21	25	19
Ba	5.3	59.4	22.2	58.7	262	199.5	164	213
Ce	10.4	14.4	16.1	22.5	23.6	50.5	67.4	50.6
Dy	3.79	4.18	4.31	5.46	3.41	5.93	7.52	4.93
Er	2.25	2.78	2.25	3.36	2.09	3.26	4.16	2.36
Eu	0.93	1.24	1.38	1.6	1.25	2.55	2.69	2.5
Ga	16.5	21.5	18.8	21.4	18.6	25.8	26	20.9
Gd	3.4	4.27	4.24	5.43	3.91	7.23	8.74	6.29
Hf	1.8	2.3	2.6	3.3	2.1	5.4	6	4
Ho	0.87	0.97	0.89	1.19	0.7	1.3	1.51	0.93
La	4.2	5.8	6.3	9.4	10.3	20.9	28.4	19.8
Lu	0.31	0.42	0.32	0.45	0.26	0.45	0.65	0.31
Nb	3.1	4.9	5.5	8.8	8.7	22.8	33.9	31.3
Ta	0.2	0.3	0.3	0.5	0.5	1.3	1.5	1
Nd	7.9	11	12.3	15.9	15	31.9	42.5	32.3
Pb					2		4	2
Pr	1.59	2.22	2.5	3.36	3.19	6.98	9.42	7.09
Rb		2.9	1.4	3.6	2.3	12.9	18.2	7.5
Sc	41	40	40	39	39	37	34	19
Sm	2.67	3.56	3.54	4.73	3.76	7.11	9.58	7.27
Sr	222	194	325	321	368	216	353	244
Tb	0.57	0.75	0.67	0.86	0.63	1.12	1.27	0.9
Th	0.36	0.51	0.41	0.86	0.7	1.79	1.81	2.45
Tm	0.36	0.4	0.35	0.49	0.29	0.46	0.58	0.33
U	0.13	0.15	0.12	0.24	0.15	0.42	0.41	0.74
V	329	420	399	458	333	548	361	245
Y	20.2	25.3	21	29.7	18	31.1	38.2	23.8
Yb	2.43	2.51	1.94	2.96	1.63	3	3.82	2.14
Zr	63	85	85	118	72	220	249	159
Cr	80	70	100	140	140	80	120	
Co	53	51	57	49	52	52	40	32
Cu	164	148	156	117	117	75	17	34
Ni	74	62	72	71	90	32	49	16
Zn	100	93	103	136	99	139	135	115

Major element compositions in wt% and trace element compositions in ppm.
Full dataset in Supplementary Data 1.

depleted as well as the enriched samples. The dated sample (BLS-73-31), corresponds to the enriched type of MPG, and indicates that the dated unit is part of the MPG magmatic event.

The ratio Tb/Yb, normalized to primitive mantle values (Sun and McDonough, 1989), can be used to show the depth of partial melt formation (Wang et al., 2002). Primitive mantle-normalized Tb/Yb ratios above 1.8 are interpreted to show melting of the mantle within the garnet stability field, whereas Tb/Yb ratios below 1.8 signify melting in shallower (<75 km) spinel lherzolite, although values close to 1.8 likely melted both garnet and spinel lherzolitic components (Wang et al., 2002) (Fig. 5e). The E-MORB-like group of the MPG falls uniformly into the spinel lherzolite field whereas the OIB-like samples form a continuous trend between the spinel stability field and the garnet stability field, with normalized Tb/Yb ratios ranging between 1.2 and 2.2. This shows that melt generation for the OIB group occurred over a range of depths.

5.4. Sm—Nd isotopes

The Nd isotope analyses are calculated using the 1998 Ma U-Pb age reported for the MPG and Minto dykes. Results are shown in Table 3. The initial Nd ratios for MPG range from $\varepsilon_{Nd}^{2.0\ Ga}$ of +2.1 to +3.8 and form a continuous trend between a depleted and an enriched endmember (Fig. 6). The dated sample (BLS-73-31) falls in the middle of this trend with an $\varepsilon_{Nd}^{2.0\ Ga}$ value of +2.56. Neodymium Depleted Mantle model ages range between 2.2 Ga and 2.3 Ga. The initial ε_{Nd} values for Minto dykes range from −3.7 to −7.8.

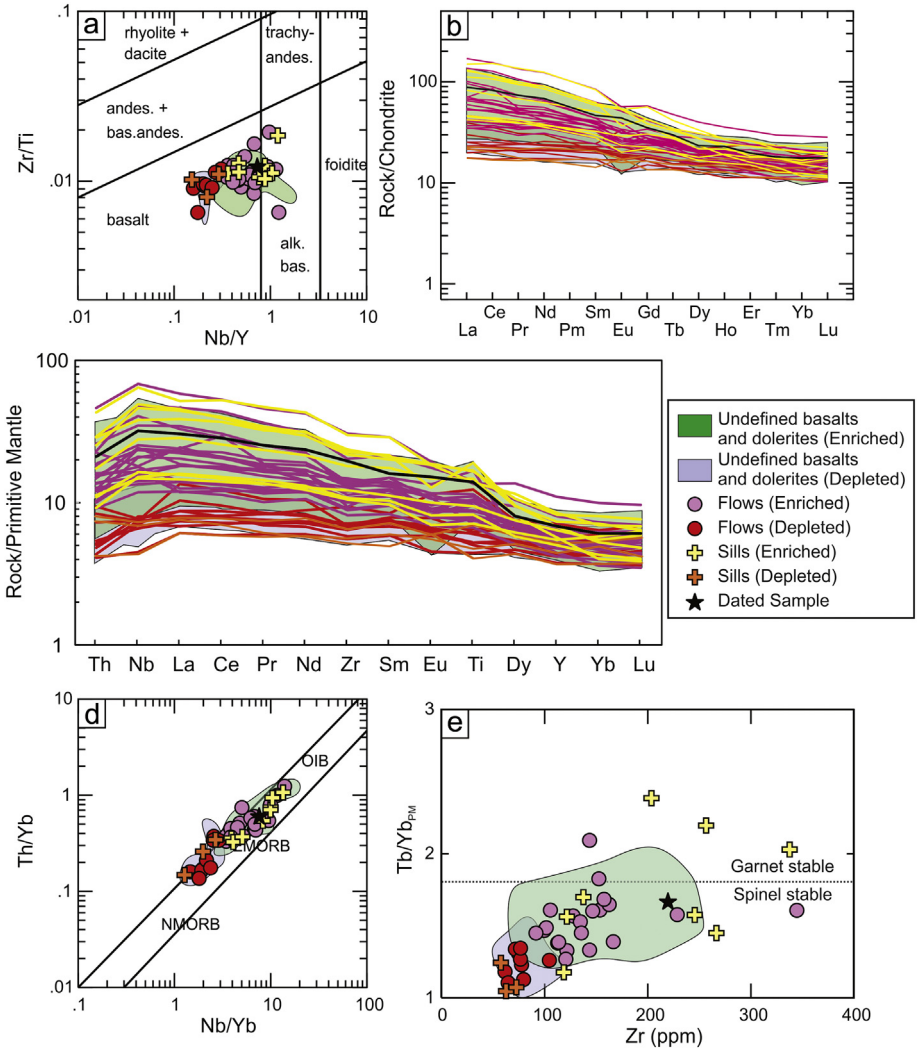

Fig. 5. Trace element geochemical diagrams for the mafic Povungnituk Group (MPG). (a)Zr/Ti vs. Nb/Y (after Pearce and Norry, 1979), (b)Chondrite normalized Rare Earth element diagram, Colors correspond to the labels in the legend, (c)Multielement diagram for incompatible elements with selected rock types, colors correspond to the labels in the legend, (d)Th/Yb vs. Nb/Yb (after Pearce, 2008), (e)Tb/Yb$_{PM}$ vs. Zr (after Wang et al., 2002). Primitive Mantle values from Sun and McDonough (1989), Chondrite values of Sun and McDonough (1989).

6. Discussion

6.1. Emplacement age of the mafic Povungnituk Group

6.1.1. Alternative interpretation of the age of the Korak sill

An U-Pb age of 2038 ± 3 Ma was obtained for the gabbroic Korak sill (Machado et al., 1993). The sill intrudes siltstones in the upper Dumas Formation, located at the base of the Povungnituk volcanic sequence. Picard (1989a), Picard, 1989b) correlates this and other diabase sills in the lower Povungnituk sediments to the main flood basalt package of the Beauparlant Formation thus implying that the Povungnituk volcanics could start at 2038 Ma. In the dataset of Picard, 1989a; Picard, 1989b), the Korak sill has not been analyzed for geochemistry and can therefore not be magmatically linked with certainty to any event.

Nilsson et al. (2010) note that the 2038 ± 3 Ma Korak sills could be instead linked to the Kangamiut-MD3LIP with dolerite ages of 2050 ± 2 Ma, 2041 ± 3 Ma and 2029 ± 3 Ma in southern West Greenland and 2045 ± 2 Ma for a dolerite in the Nain Province. These have been interpreted to represent components of a single, areally extensive, radiating dyke swarm that signaled the arrival of a mantle plume centred on what is presently the western margin of the North Atlantic craton (NAC) (Nilsson et al., 2010), and at this time the NAC is interpreted to have been located further north adjacent to the NE margin of Superior craton, at a minimum distance of approximately 250 km from the Korak sill location (see Fig. 5 in Nilsson et al. (2010). More detailed work on the constraint of the location of the NAC is required to access the exact distance between a ca. 2040 plume centre and possible Korak sill emplacement.

Table 3
Summary of the Sm—Nd results.

Formation	Sample	Sm (ppm)	Nd (ppm)	$^{147}Sm/^{144}Nd$	$^{143}Nd/^{144}Nd$	$\varepsilon_{Nd}^{1998\ Ma}$
MPG	BLS 31 73	7.67	32.98	0.1407	0.512031	2.56
MPG	BLS 41 73	6.08	25.15	0.1463	0.512111	2.67
MPG	BLS 55 73	3.33	10.85	0.1855	0.512685	3.8
MPG	BLS 180 73	5.92	26.63	0.1345	0.511925	2.06
MPG	BLS 183 73	3.71	15.11	0.1483	0.510216	3.24
MPG	BLS 197 73	3.40	11.44	0.1798	0.512590	3.42
MPG	BLS 264 73	8.89	40.44	0.1329	0.511902	2.02
MPG	SAB87-179	3.83	15.29	0.1513	0.512171	2.56
Minto	BXA91-7904	6.87	30.06	0.1381	0.511677	−3.73
Minto	BXA91-8103	6.91	31.57	0.1324	0.511559	−4.57
Minto	BXA91-8203	6.15	29.79	0.1248	0.511290	−7.87
Minto	BXA91-8406	4.81	20.38	0.1426	0.511668	−5.06

2σ uncertainties of $^{147}Sm/^{144}Nd$ are 0.5%.
2σ uncertainties of $^{143}Nd/^{144}Nd$ 0.000011, given by the reproducibility of the standart.
ε_{Nd} values are calculated relative to a present day $^{143}Nd/^{144}Nd$ CHUR values of 0.512638.

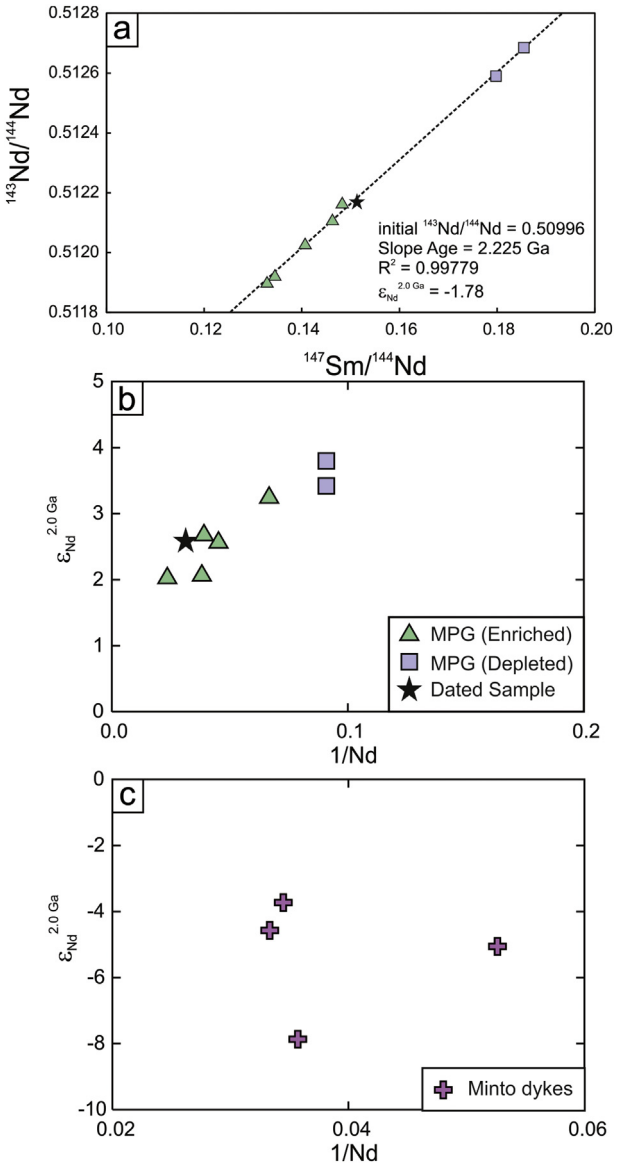

Fig. 6. Sm–Nd isotopes of mafic Povungnituk Group (MPG) samples and Minto dykes.

6.1.2. Age of Povungnituk Group flood basalts

The new ca. 1998 ± 6 Ma maximum age that we have obtained for the upper Povungnituk Group represents the first age on mafic rocks included into the stratigraphy of the Beauparlant Formation. It is significant that the geochemistry of the dated intrusive sample matches the associated MPG chemistry (Figs. 4, 5). The age is obtained from a dolerite sill at the top of the exposed Povungnituk Group succession and therefore provides a new minimum age for Povungnituk magmatism.

This age is similar to the 1991 ± 2 Ma age reported by Machado et al. (1993) from a small granodiorite intrusion which cross-cuts Povungnituk Group pillow basalts and represents a minimum age for the formation of the Povungnituk Group.

Only rare dolomite and semipelite occurrences (described as "volumentrically subsidiary intercalated" (Mungall, 2007) or "very minor quantities of interflow sediment" (St-Onge et al., 1992) are present within the Povungnituk flood basalts led to the interpretation by St-Onge et al. (1992) that the main part of the MPG was emplaced in a relative short time, an interpretation that would also be consistent with the Korak sills belonging to a different LIP. The short duration of emplacement of the Povungnituk is also supported by Mungall (2007), who interprets the Beauparlant Formation to be a single sequence ~3 km in original thickness. This is comparable to other LIP events, like the Siberian Trap (Burgess and Bowing, 2015) and Deccan Trap (Schoene et al., 2015) which also lack significant interflow sediments and for which precise U—Pb dating indicates a duration of less than a few million years.

The rhyolite sample obtained from the alkaline rocks at the Cecilia and Kenty lakes localities has been dated at 1958 ± 3 Ma (Parrish, 1989). The localities are interpreted to represent an association of an alkaline volcanic series with the continental tholeiites and sediments of the Povungnituk Group via a volcanic island on a rifted continental margin (Gaonac'h et al., 1992 and are not immediately linked to the main flood basalt pulse. An initial $\varepsilon_{Nd}^{2.0Ga}$ value of +0.4 on the dated rhyolite sample further indicates minor contamination, which probably occurred during ponding of mafic magma at the crust-mantle interface during rifting (Francis et al., 1983; Hegner and Bevier, 1991).

Given the chemical homogeneity of the MPG regionally (Modeland et al., 2003; this study), and the lack of significant sedimentation or alteration horizons (Mungall, 2007; St-Onge et al., 1992), it is possible that large components of the MPG may have formed over a short duration. Therefore we provisionally interpret our age of 1998 ± 6 Ma as representative of the main phase of volcanism.

6.2. Link with coeval regional units and recognition of a 1998 Ma Minto-Povungnituk LIP

The new age constraints suggest links with a number of mafic magmatic units in the Quebec promontory of the Superior craton (Fig. 7). The Minto dykes in the interior of the craton have a U—Pb baddeleyite-zircon age of 1998 ± 2 Ma (Buchan et al., 1998). The Lac Shpogan dykes of the James Bay area of the eastern Superior craton have been recently correlated with the Minto dykes based on a U—Pb baddeleyite age of 1999 ± 2 Ma (Hamilton et al., 2016).

An identical age was obtained from the Watts Group (Purtiniq) ophiolite in the northern Cape Smith Belt (Parrish, 1989; Scott et

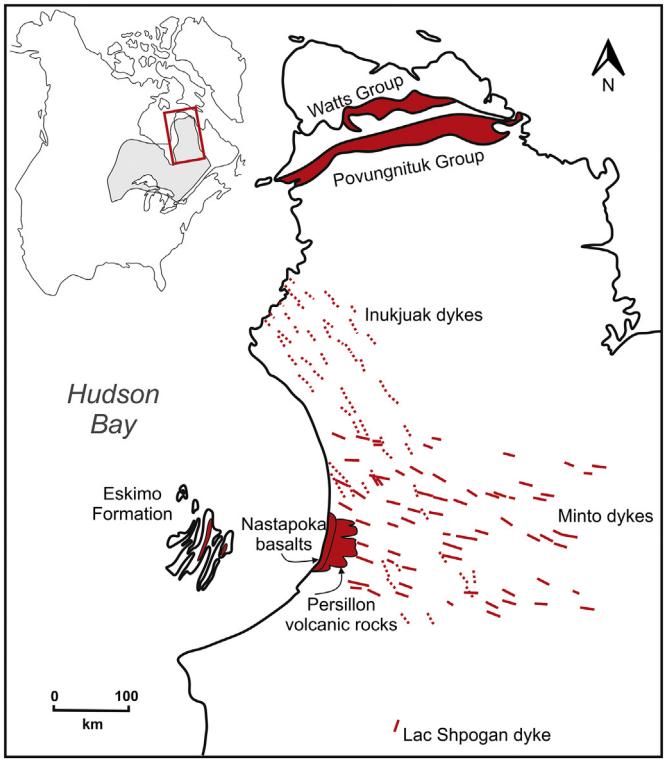

Fig. 7. Map showing coeval magmatic units of the ca. 1998 Ma Minto-Povungnituk large igneous province. Inspired by Chandler (1984); Buchan et al. (1998); St. Onge et al. (2004); Baragar (2007); Maurice et al. (2009).

al., 1999). The Watts Group comprises layered ultramafic and mafic rocks, clinopyroxenite intrusions, sheeted mafic dykes and gabbros, and pillowed and massive mafic volcanic rocks intruded by rare felsic sills and dykes (Scott et al., 1991, 1999; St-Onge et al., 1992). The rocks that comprise the ophiolite are separated from the underlying sedimentary rocks by a south-verging thrust fault. Two samples of Watts Group mafic cumulates were dated using zircons. In a metagabbro, zircons yield a U—Pb age of 1998 ± 2 Ma, whereas in a metamorphosed anorthositic layered gabbro, two types of zircons are present. Igneous cloudy grains are 1995–2000 Ma whereas clearer overgrowths are 1977 ± 3 Ma, perhaps related to seafloor metamorphism (Scott et al., 1999).

In recent years, the use of precise U—Pb geochronology has been led the recognition of many new LIPs and revealed their wide distribution within continental blocks (e.g. Baratoux et al., 2019; Ernst et al., 2013; Samal et al., 2019). The standard approach has become to correlate intraplate units in a region on the basis of their U—Pb age matches and then to subsequently use geochemistry (mainly trace elements and isotopes) to interpret the distribution of distinct geochemical types. Geochemistry on its own has been shown to be an unreliable guide to identifying units that belong to the same LIPs, given that many LIPs exhibit multiple geochemical types (Ernst, 2014).

Therefore, the overlap in age determinations as discussed above suggests that a 1998 Ma magmatic event was widespread in and around the Quebec promontory, the eastern part of the Superior craton, covering an area over 400,000 km^2(Fig. 7). An additional unit, the Eskimo volcanics, are correlated on the basis of paleomagnetism with the dated Minto dykes (Buchan et al., 1998), and together all these linked units are referred to as the 1998 Ma Minto-Povungnituk LIP. Additionally, the Nastapoka basalts in the Richmond Gulf area have been paleomagnetically linked to the Minto and Lac Shpogan dykes (Buchan et al., 1998), and the Persillon Formation in the Richmond Gulf area has been geochemically linked to the Eskimo Formation and the undated Inukjuak dykes (Legault et al., 1994).

6.3. Differences between chemistry of northern and southern portions of the Minto-Povungnituk LIP

The geochemistry of the different units within this Minto-PovnungnitukLIP reveals regional compositional and isotopic differences that split the proposed LIP into “northern” and “southern” groups that were emplaced at approximately the same time.

6.3.1. Northern magmatism (Povungnituk – Watts Group connection)

Two geochemically distinct magmatic suites have been identified within the layered mafic and ultramafic rocks of the Watts Group (Fig. 8) on the basis of major and trace element abundances and Nd isotopic composition (Hegner and Bevier, 1991; Scott et al., 1991, 1999). AMORB-like suite is tholeiitic and characterized by low abundances of elements such as Ti, Zr, Y, and the light REE, has La/Sm$_{PM}$ ~ 1.1, and has $\varepsilon_{Nd}^{2.0\ Ga}$ values that range from +3.0 to +4.7 (Hegner and Bevier, 1991). Both of the aforementioned gabbro samples for which U—Pb ages were determined belong to this suite.

The second suite is referred to as tholeiitic OIB-like(Scott et al., 1991, 1999). It has incompatible element abundances that are enriched relative to MORB(Scott et al., 1991), normalized incompatible element patterns peak at Nb and Ta as do modern OIB(Salters and Stracke, 2004), and $\varepsilon_{Nd}^{2.0\ Ga}$ values that range from +2.7 to +3.1 (Hegner and Bevier, 1991). The absolute age of this suite has not been directly determined but has been assumed to also be ca. 2000 Ma. The sheeted dykes of the two geochemical groups are indistinguishable from each other in outcrop and do not show consistent cross-cutting relationships, suggesting that their emplacement was coeval with the cumulate rocks (Scott et al., 1999).

Stratigraphy along the three traverses sampled for the MPG vs. diagnostic element ratios show no correlation with increasing stratigraphic level. Instead, they vary between the two geochemical signatures (Fig. 2). The clearest distinction is seen in the westernmost traverse (Fig. 2, western traverse). This pattern across the stratigraphy is in accordance

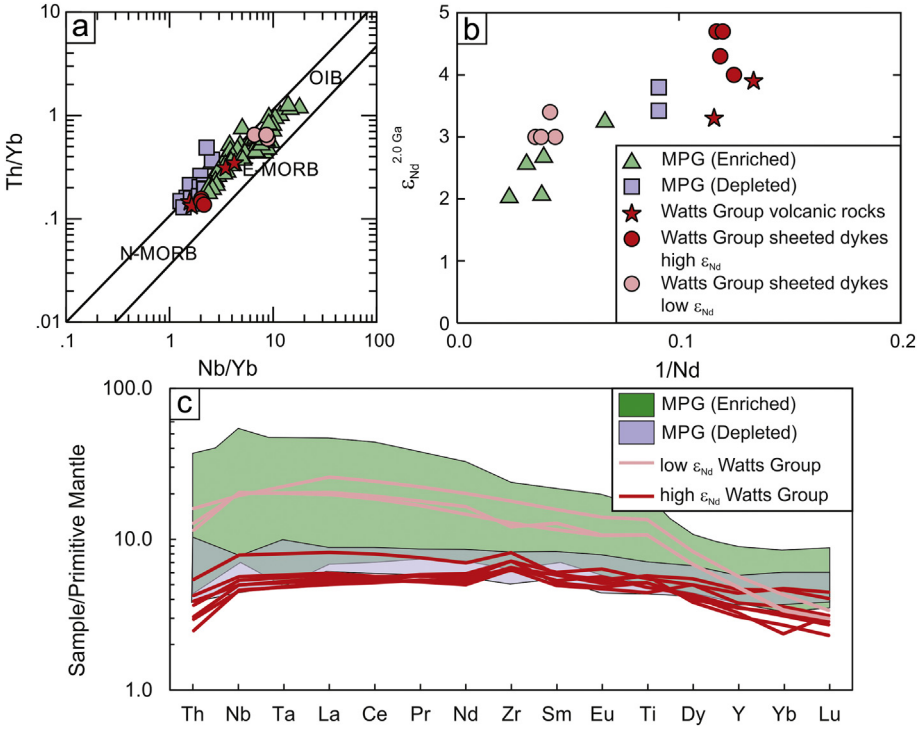

Fig. 8. Geochemical comparison of *E*-MORB and OIB suites for the mafic Povungnituk Group (MPG) and the low and high ε_{Nd} Watts Group. Primitive mantle values from Sun and McDonough (1989).

with magma being derived alternately from two staging chambers (Lightfoot and Hawkesworth, 1997).

Two distinct mantle sources (MORB- and OIB-like) with different isotopic compositions were involved in the generation of the Watts Group (Purtuniq) ophiolite. Each source produced a suite of cumulate rocks and sheeted mafic dykes. The first one is a trace element depleted source similar to MORB. Scott et al. (1991) interpreted this source to have been long-lived and to have been enriched metasomatically immediately prior to melt generation to form the more enriched OIB-like suite.

The two distinct geochemical groups outlined by the Watts Group (Scott et al., 1991, 1999) correlate well with the two groups in the MPG. All samples can be classified as basalts. In a diagram of Th/Yb vs. Nb/Yb (Pearce et al., 2008) the Watts sheeted dykes groups overlap with the two endmembers (*E*-MORB and OIB-like) of the MPG, whereas the volcanic rocks of the Watts Group overlap with the E-MORB endmember of the MPG(Fig. 8). This behaviour is apparent for both major and trace elements. An exception is the Gd/Yb ratios. The low ε_{Nd} sheeted dyke samples of the Watts Group generally show the highest Gd/Yb ratios. This indicates that melting of the low εNd member of the Watts Group might have occurred at an even greater depth than for the majority of the OIB-like samples of the MPG.

Another option would be that slightly different material has been melted to produce the Watts Group compared to the MPG magmas. Several lines of evidence indicate that the modern mantle contains a significant fraction of pyroxenites (Schulze, 1989). These may play an important role in controlling the chemical variability of mantle-derived melts (Sobolev et al., 2007) and have been shown to be incorporated into OIB(Kogiso et al., 2003; Kogiso and Hirschmann, 2006; Petermann and Hirschmann, 2003) and MORB(Lambart et al., 2009). In a diagram of Ce/Yb vs. Yb it is evident that, instead of different melting depths, pyroxenite melting could have been involved in the generation of the Watts Group, resulting in the observed HREE signature (Fig. 9). This would open the possibility that the northern domain has been melted at the same depth but definitive constraints on the depth of melting cannot be made.

Broadly, the Watts Group Nd isotope values overlap with those of MPG. The low ε_{Nd} sheeted dykes and volcanic rocks of the Watts Group have values that overlap with but tend to be more depleted than MPG (+3 to +6.1). They form no trend towards less depleted $\varepsilon_{Nd}^{2.0\ Ga}$ values but correlate well with the trend shown by MPG in a diagram of $\varepsilon_{Nd}^{2.0\ Ga}$ vs. 1/Nd. The low ε_{Nd} sheeted dykes of the Watts Group roughly overlap with the OIB-like samples of the MPG. Overall, the Watts Group displays the same mixing trend between two distinct mantle endmembers as the MPG.

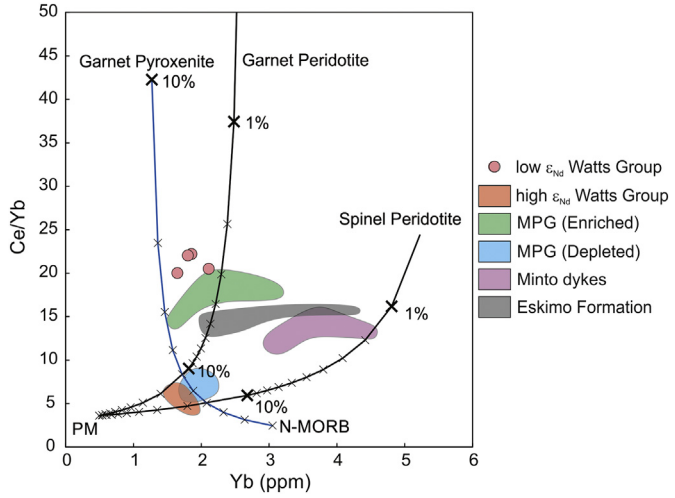

Fig. 9. Ce/Yb vs. Yb concentration showing non-modal, batch partial melting models (Shaw, 1970) for spinel peridotite, garnet peridotite (black lines), and garnet pyroxenite (blue line). For peridotite models, starting compositions assume PM concentrations; modal abundances, and D values from Salters and Stracke (2004). For the garnet pyroxenite model, starting composition is N-MORB with modal abundances, and D values from Petermann et al. (2004).

6.3.2. Southern magmatism (Minto – Eskimo connection)

The geochemistry of the Minto dykes does not show either of the two distinct groups observed in the MPG and Watts Group samples (Fig. 10). The Minto dykes all plot in the basalt field shown in a Zr/Ti vs. Nb/Y (Fig. 10a) diagram and all plot in the field described for plate margin basalt in a diagram of Zr/Y vs. Ti/Y (Fig. 10b).

In a Th/Yb vs. Nb/Yb (Fig. 10c) diagram half of the samples plot within the mantle array, overlapping with the E-MORB field and the transitional samples described for the MPG. Although showing similar La/Yb ratios, Minto dyke samples have slightly higher La/Sm_C ratios against La/Yb_C than MPG(Fig. 10d). Two samples plot slightly outside of the mantle array showing that interaction with crustal material might have been involved in their formation. These samples also display a negative Nb-anomaly in primitive mantle-normalizedmulti-element diagrams (Fig. 10e). Minto dyke REE compositions are slightly different from compositions observed in the MPG.

The most significant geochemical difference between Minto dykes and MPG can been seen in their Nd isotopes. Minto dykes have initial $\varepsilon_{Nd}^{2.0\ Ga}$ values that are highly negative (−3.7 to −7.9) in contrast to the positive $\varepsilon_{Nd}^{2.0\ Ga}$ values (+2.0 to +3.8) for the MPG (Fig. 11a). Therefore, although matching in age and interpreted to belong to the same LIP (as discussed above), MPG and Minto dykes must have been fed from vastly different sources or have undergone different magmatic evolution processes since magma segregation from the mantle. To assess if this spread in Nd-isotope geochemistry is source-related or related to magmatic processes such as mixing or assimilation, we have to observe how these Nd-isotopic differences correlate with differences in major and trace element ratios. As illustrated in Fig. 11a the spread in Nd-isotopic composition is negatively correlated with Mg#, meaning the lower $\varepsilon_{Nd}^{1998\ Ma}$ values of the Minto dykes are correlated with higher Mg#. If the samples would have been contaminated by felsic rocks during fractionation, the lower ε_{Nd} values would be correlated with lower Mg#.

Explanations for such observations have been listed by Devey and Cox (1987) in their study of the 66 Ma Deccan Traps LIP event (India). They concluded that either coincidental causes (contaminants become less available over time, or changes of flow rate in dykes) need to be constrained or that magmatic temperature is the controlling influence for the contamination signature. The correlation between Mg-number and Nd isotopes is then directly linked to the magma source before dyke emplacement, as crustal contamination fades out because themagmas become too cool. This is essentially an assimilation-equilibrium crystallization (AEC) process, which demands the suppression of fractional crystallization (Devey and Cox, 1987). Hence, even if a fractionation chamber existed, it cannot be the main site of contamination. Two plausible explanations for this have been proposed.

The existence of magma chambers with high surface-to-volume ratios, which allow a large surface area of magma to come into contact with the country rock, and so permit partial fusion of the more acidic or volatile-rich portion of the crust over relatively short time scales (Huppert and Sparks, 1985) or a chamber located within the upper part of the mantle rather than the crust, where any interaction with wall rocks did not result in identifiable isotopic or trace element signatures (Devey and Cox, 1987). In both cases any measurable contamination would occur during magma ascent in the crust rather than in a magma chamber. Contamination is then dependent on the type of flow in the magma conduit. Under laminar flow the initial formation of a chilled margin around the conduit would shield later magmas from contamination. Huppert and Sparks (1985) and Campbell (1985)

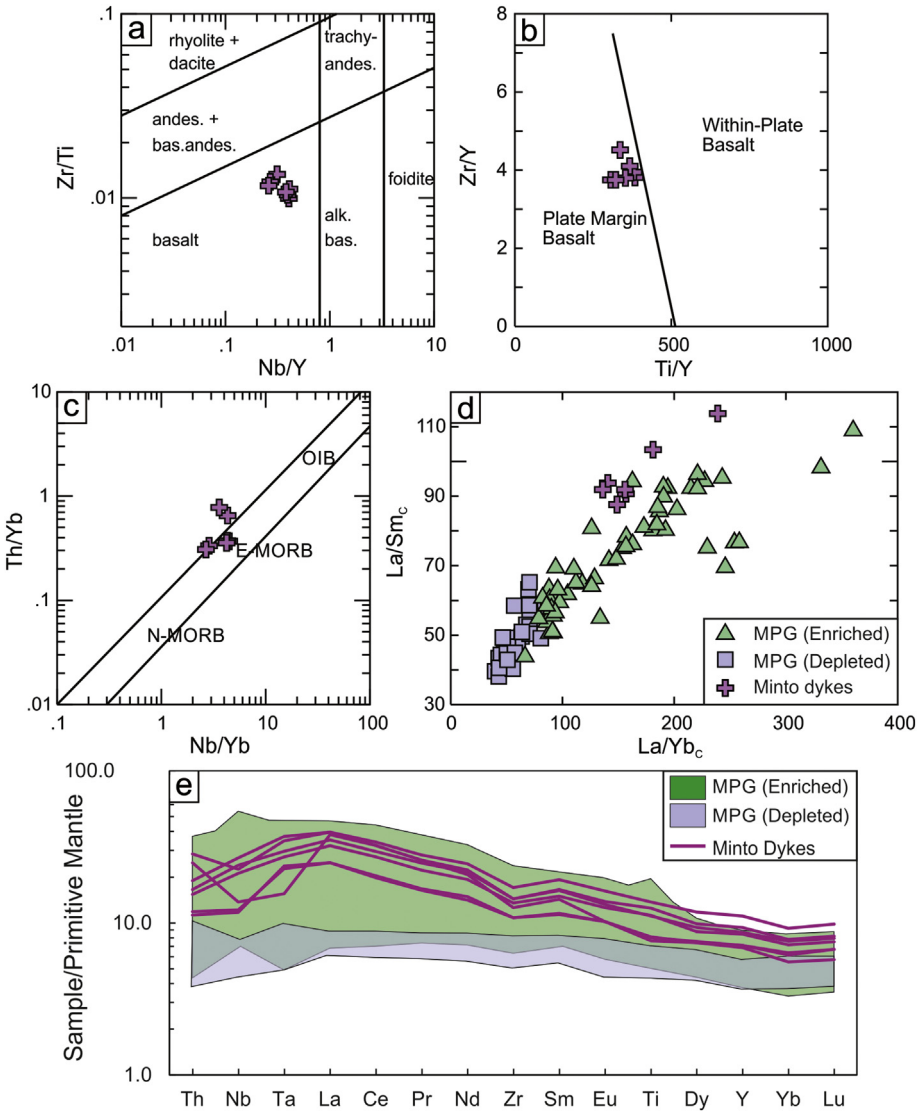

Fig. 10. Trace element geochemical diagrams for the Minto dykes compared with the mafic Povungnituk Group (MPG). (a)Zr/Ti vs. Nb/Y (after Pearce and Norry, 1979). (b)Zr/Y vs. Ti/Y (after Pearce and Gale, 1977). (c)Th/Yb vs. Nb/Yb (after Pearce, 2008). (d)La/Sm$_C$ vs. La/Yb$_C$, chondrite values from Sun and McDonough (1989). (e)Multi-element diagram for immobile elements, Primitive Mantle values from Sun and McDonough (1989).

have shown however, that basaltic magma can ascend turbulently if the flow rate is sufficiently high (>25 m^2/s) and the conduit width great enough (>3 m in primitive magmas). Under such circumstances a chilled margin is less likely to form initially, or is subsequently remelted. This brings turbulently ascending magma into continual contact with surrounding country rock and so the most fusible wall rock components can be melted and incorporated into the magma. Such a progress will lead to the most primitive (i.e. hottest magmas) becoming the most contaminated.

Basaltic magmas, such as Minto dykes, have a low enough viscosity such that high flow rates along wide dykes would create turbulence during motion. With widths between 13 and 60 m, most of the Minto dykes greatly exceed the width requirements for turbulent flow of tholeiitic basalts given by Huppert and Sparks (1985). Although thinner dykes can be simply offshoots of thicker dykes, the thinner Minto dykes (samples 7904 and 8003; Ernst and Buchan, 2010) would have ascended under laminar flow conditions and show the least contaminated Nd-isotopic signature ($\varepsilon_{Nd}^{2.0\ Ga} = -3.73$) in support of the proposed model.

Primary paleomagnetic directions have been obtained from the Minto and Lac Shpogan dykes (Buchan et al., 1998). Their paleopole is similar to pre-fold paleopoles reported from the Eskimo volcanic rocks of the Belcher Islands and the Nastapoka basalts of Richmond Gulf (Schmidt, 1980; Schwarz and Fujiwara, 1981). The Persillon volcanic rocks of Richmund Gulf and the Inukjuak dykes have also been correlated on the basis of geochemistry with the Eskimo Formation (Legault et al., 1994), suggesting that they may also belong to the ca. 1998 Ma Minto-Povungnituk event. Given the limited data available and the absence of available ages, a correlation with the Persillon volcanic rocks and the Inukjuak dykes remains tentative.

The Eskimo volcanic rocks have geochemical signatures that are distinct from those of the MPG. Previous work on the Eskimo Formation by Chauvel et al. (1987) and Legault et al. (1994) provided isotopic compositions and detailed major and trace element chemistry, respectively. Both studies concluded that Eskimo Formation basalts are evolved and unlikely to represent direct partial melts of the upper mantle. Both studies argued that assimilation-fractional crystallization (AFC) is the controlling process during the formation of the Eskimo Formation due to the negative correlation of Nb/Zr with Zr.

Reanalyzed major and trace element data on the Eskimo Formation have been published by Ernst and Buchan (2010). The data differ drastically in trace element values from the results published by Legault et

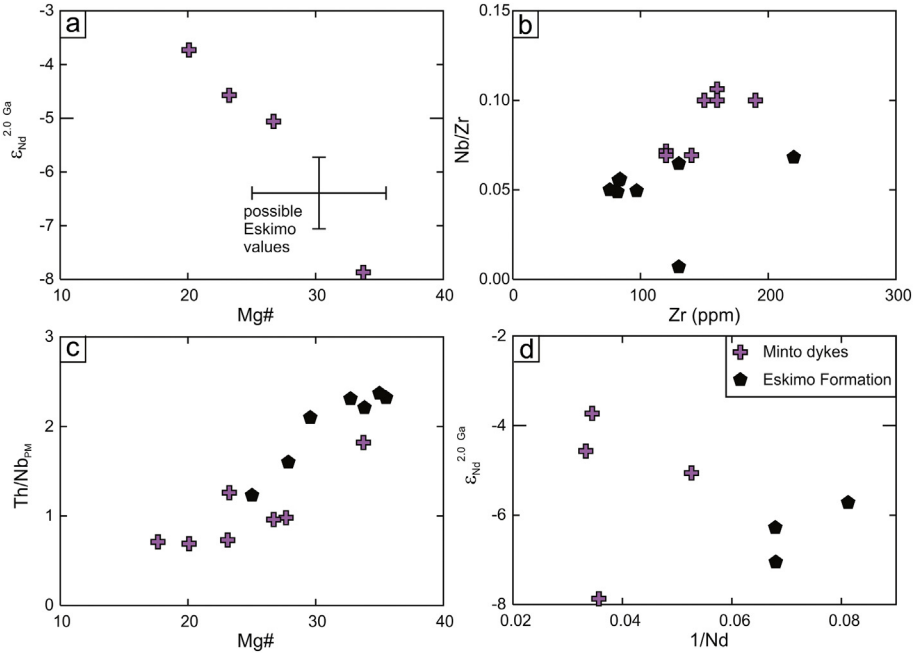

Fig. 11. Geochemical diagrams for Minto dykes and Eskimo basalts. Primitive Mantle values from Sun and McDonough (1989).

al. (1994). The same element ratio diagrams as previously mentioned (Nb/Zr vs. Zr) now show the exact opposite and show a positive correlation between Nb/Zr and Zr (Fig. 11b). Data from Ernst and Buchan (2010) were determined by fused disk wavelength dispersive X-ray Fluorescence (XRF) for major elements and by Inductively Coupled Plasa – Emission Specrometry (ICP-ES) as well as Inductively Coupled Plasma – Mass Spectrometry for trace elements concentrations. In contrast, the trace element data in Legault et al. (1994) were obtained by XRF and INAA. Niobium concentrations below 10 ppm for the Eskimo volcanic rocks are below the detection limit of XRF, casting doubt on the Nb/Zr ratios of Legault et al. (1994).

The precision of the Ernst and Buchan (2010) data was supported by 26 duplicate measurements and 18 measurements of an internal CANMET standard (TDB-1) that were interspersed in the sample stream, and all samples were analyzed for the same elements at the same laboratories, resulting in an internally consistent dataset. For the present manuscript the Ernst and Buchan (2010) data on the Eskimo volcanic rocks are used for comparison with the Minto dykes. Using these data, indicators of crustal assimilation are now correlating with more primitive samples and fall on linear trends with the Minto dykes. To avoid the effects of element mobility we used a ratio of Th/Nb to show the higher amount of crustal assimilation (high Th/Nb) in the more primitive rocks (Fig. 11c). $\varepsilon_{Nd}^{2.0\ Ga}$ values for the Eskimo Formation range from −5.7 to −7.0 (Chauvel et al., 1987). Unfortunately, published data are only available with Nd and Sm concentrations and prohibit a detailed geochemical comparison with the Minto dykes to determine their relationship. Nevertheless, a plot of $\varepsilon_{Nd}^{2.0\ Ga}$ vs. 1/Nd shows a negative correlation in agreement with the proposed AEC processes (Fig. 11d). The chemistry of the two widest Minto dykes (60 m and 17 m) directly overlap with the Eskimo volcanic rocks (Fig. 11b and c) and suggest that these might represent feeders for the Eskimo volcanic suite.

Assessing the extent of crustal contamination proves complicated. Huppert and Sparks (1985) showed that turbulently-ascending tholeiitic dykes can only assimilate around 5% crustal rocks. Using average Nd-isotopic values for Superior craton basement (Chauvel et al., 1987) as a contaminant does not yield the observed geochemical signatures. Either contaminants with more depleted Nd-isotopic signatures were involved or higher Nd concentrations are necessary to explain the observed data. Neodymium concentrations exceeding 100 ppm have been documented on several analyses of felsic basement in the Superior craton (Énergie et Ressources Naturelles Québec, 2018). These high Nd concentrations would be sufficient to contaminate Minto dykes with Archean lower crust, with $\varepsilon_{Nd}^{1998\ Ma}$ of −12 (Chauvel et al., 1987), to produce Eskimo basalt compositions with <5% contamination.

6.4. Bilateral asymmetry of Minto-Povnungnituk LIP: possible models

An interesting feature of the Minto-PovungnitukLIP recognized in the present research is the distinct “northern” and “southern” domains. The northern domain consists of the MPG and the Watts Group ophiolite. The southern domain consists of the Minto dykes and the Eskimo basalts. The Minto dykes therefore do not seem to be feeders for the MPG, but instead seem to be feeders only for the Eskimo volcanic suite.

A continental rift zone located beneath northern Hudson Bay (present location) between 2040 Ma and 1998 Ma associated with uplift in the Superior craton has been proposed by Halls and Davis (2004), parallel to the orientation of the Minto dykes (Fig. 7). One possible model is that this rifting event could have been induced by the arrival of a mantle plume (cf, Midcontinent rift volcanism (Hollings et al., 2006; Nicholson and Shirey, 1990)). Plume-related magmatism in the northern domain of the LIP is supported by the OIB component of the MPG and Watts Group. A potential plume centre could be associated with the uplift determined by Halls and Davis (2004) and would be located beneath Hudson Bay (Fig. 7).

It can be inferred that the Minto dykes trend away from this plume centre and were potentially fed from a source in the southern domain (Fig. 7), while the MPG (and Watts Group) were linked to sources in the northern domain. Fig. 12 shows hypothetical scenarios that could explain how the different magmatic domains of the Minto-PovungnitukLIP were fed. Two possible models for generating this bilateral compositional asymmetry are considered below.

6.4.1. Lithospheric effect

Different lithospheric domains have been hypothesised by Maurice et al. (2009) to underlie the northern vs. southern intrusions of the plume centre region. The “northern side” would be underlain by thinned Superior craton lithosphere. The “southern” domain would be underlain by older and thicker lithosphere. In an extensive comparative study, Maurice et al. (2009) showed that a change in the chemistry of

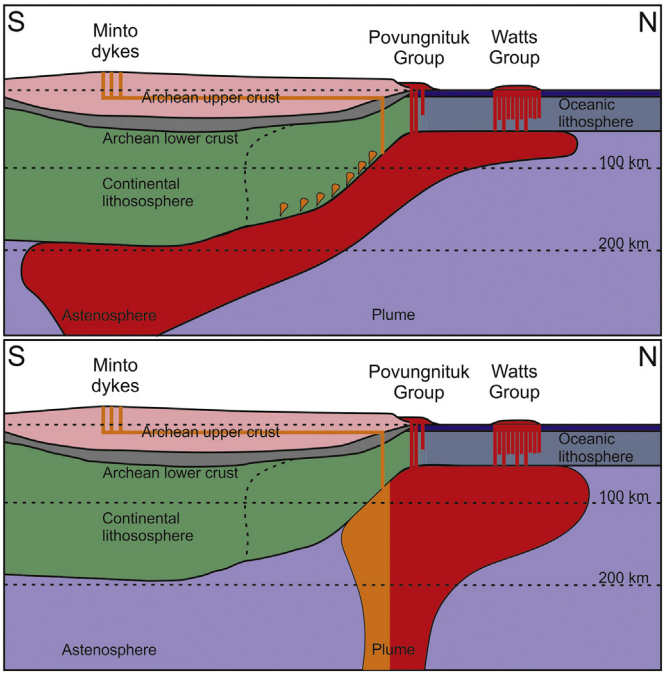

Fig. 12. Schematic sections showing the two possible models of the 1998 Ma Minto-Povungnituk LIP, as discussed in the text (modified after Maurice et al., 2009).

dyke swarms occurred after 2030 Ma in the northeastern part of the Superior craton. They concluded that part of the lithospheric mantle delaminated from the northeastern Superior craton at 2030 Ma, and upwelling asthenospheric mantle underwent partial melting to produce the different geochemical signatures observable in dykes emplaced after 2030 Ma in that region. This could explain the geochemical and isotopic differences observed between the northern and the southern domains of the Minto-Povungnituk event, with the northern domain lacking signatures of the Superior craton lithosphere, whereas the southern domain still ascended through thick lithosphere creating the observed enriched signatures. In their study, Maurice et al. (2009) implied that all dyke swarms ascended vertically through the crust and were created by melting of the underlying lithospheric mantle. However, lateral dyke injection from the plume centre region into the craton may be more common, especially in areas with thick lithospheric roots. Dykes can only propagate upwards under conditions of positive buoyancy and will tend to propagate laterally once a level of neutral buoyancy is approached (Lister, 1991; Lister and Kerr, 1990; Wilson and Head, 2002). Lateral injection of dyke swarms away from a mantle plume centre has been shown for the Mackenzie and other swarms (Baragar et al., 1996; Ernst, 2014; Sandeman et al., 2014).

The lithospheric thickness of the Superior craton is believed to exceed 140 km south of the Cape Smith Belt and to be up to 170 km at the location of the Minto dykes (Fig. 2 in Maurice et al., 2009). The magmatic inactivity of the Ungava Peninsula after the emplacement of the Paleoproterozoic dyke swarms and Circum-Ungava belts implies that the present structure of its underlying mantle has not been affected by younger events (Maurice et al., 2009). This coincides with observations that the northeastern Superior Province represents an Archean terrain with a thick cratonic keel older than 2.6 Ga (Bédard et al., 2013; Boily et al., 2009; Harris and Bédard, 2014), a notion that is further supported by the inferred occurrence of Archean diamondiferous kimberlites in the western Superior craton (Kopylova et al., 2011). Basaltic melt generation at depths >100 km is unlikely and even if melt was produced it would reflect melting in the garnet peridotite stability field (e.g., higher Gd/Yb ratios resulting from residual garnet) (White and McKenzie, 1995). Therefore, it is unlikely that melting occurred beneath the thick root of the craton. Instead melting likely occurred closer to the plume centre on the side of the craton, and that dykes propagate laterally into the craton from this plume centre. Interaction with Superior craton lithosphere would then occur at the cratonic margin beneath Hudson Bay, near the inferred plume centre along the projection of the Minto dyke trend.

A possible explanation for the melt generation, still involving a lithospheric signature, would include the plume rising up beneath the Superior craton and gradually spreading along the lithospheric keel (e.g., Sleep, 1996). On its ascent, the plume can then gradually melt parts of the lithosphere and flow towards a shallow magma chambers surrounding the plume centre. From there a sub-swarm of dykes could intrude into the Superior craton creating the Minto dykes (Fig. 12). The injection of individual sub-swarms surrounding plume centres has been suggested by Baragar et al. (1996) and Blanchard et al. (2017).

6.4.2. Distinct or zoned plumes

Another explanation for the difference in compositions between the northern domain (MPG and Watts Group) and southern domain (Minto dykes and Eskimo basalts) is, they originate from two different neighboring mantle plumes. Numerical modelling for determining coeval plume spacing is strongly affected by boundary layer heterogeneities and therefore have not been successful (Sleep, 1992; Wüllner and Davies, 1999). However several examples throughout Earth's history show that roughly coeval neighboring plumes exist. These include the 2.48–2.45 Ga Matachewan and 2.51 Mistassini plume centers along the eastern margin of the Superior craton, which are 800 km apart and the 2.23 Ga Malley and 2.21 Ga MacKay plume centers along the eastern margin of the Slave craton, which are >500 km (e.g., Buchan et al., 2012; Ernst and Bleeker, 2010). Based on these examples, coeval plume centers can be as closely spaced as 500–800 km.

Alternatively, we consider the possibility of two distinct types of deep mantle material rising in a single plume representing chemical zonation of the plume source. The deep mantle currently hosts one minor and two major regions of low shear wave velocity (LLSVP) that are inferred to represent slab graveyards. The edges of the LLSVPs have been associated with the formation of mantle plumes for the past 300 myr (Torsvik et al., 2010, 2014). Weis et al., 2011 and Harrison et al., 2017 proposed the Hawaiian plume rising along the edge of the LLVSP and mechanically removing fragments of the LLSVP and carrying them upward. They attribute the Kea compositional component to the plume and the Loa compositional component to the LLSVP (Harrison et al., 2017; Harrison and Weis, 2018). These components ascended on opposite sides of the plume and reflect the structure of the underlying deep mantle. This process has been shown to be possible, if thermal heterogeneity outweighs chemical heterogeneity in the source region (Jones et al., 2016). Utilizing the Hawaiian model, we consider the idea that the northern vs. southern compositional domains of the Povungnituk-MintoLIP are related to ascent of different mantle material on opposite sides of the plume. Upon arrival at the base of the lithosphere the plume would spread out in opposite directions from the plume centre (Fig. 12). Partial melting of these distinct mantle sources would lead to mafic compositions with the distinct features of the Povungnituk-Watts (northern) vs. Minto-Eskimo (southern) domains.

If we consider the northern vs. southern domain chemistry in the Minto-PovungnitukLIP to have originated in the deep mantle, the Povungnituk-Watts component (northern domain) would be linked to ambient deep mantle, whereas the Minto-Eskimo (southern domain) composition has isotopic characteristics that represent an enriched source (e.g., slab graveyard). It would be difficult to achieve upwelling of a plume from a slab graveyard causing complications for the two-plume model, but can be satisfied in a single zoned plume model.

The potential implications of the Minto-PovungnitukLIP being related to ambient lower mantle and LLSVP are intriguing. A key issue is the potential for sufficiently enriched εNd compositions ($\varepsilon_{Nd}^{1998\ Ma} = -4$) in a slab graveyard at 2 Ga. Differentiated material needs to be

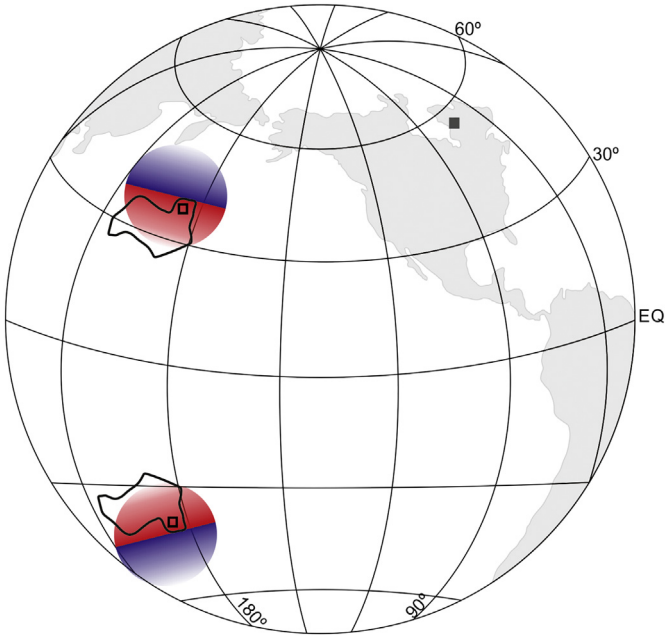

Fig. 13. Globe showing the paleo-latitude of the Superior craton at the time of Minto dyke emplacement (ca. 1998 Ma) referenced to present day geography (after Buchan et al., 2007). Minto dykes location is shown as squares. Open squares represent the paleomagnetic reconstruction and the closed square represents its current day location. Coloured fields indicate the deep mantle structures inferred to explain the bilateral symmetry of the Minto-Povungnituk LIP. See discussion in text.

subducted early in Earth's history to give sufficient time to develop the observed isotopic signatures.

In summary, various assumptions need to be made that cannot be further tested with the currently available dataset, namely that the LIP represents a)a single plume, b)is sourced from different lower mantle sources and has not been influenced more by upper mantle or lithospheric processes and c)is ultimately derived from the LLSVP region.

6.4.3. Constraining the existence and location of LLSVPs in the Precambrian

Two models have been proposed for the origin of the different geochemistries between the northern and the southern domains of the Minto-Povungnituk LIP. Melting of Superior craton continental lithosphere created magmas (southern domain) that are geochemically different from the melts produced by mixing of the melting plume head with adjacent depleted mantle (northern domain). Alternatively, the bilateral chemistry of the Minto-PovungnitukLIP can be explained by melting of different plume head material that had been sourced from different deep mantle domains and has been brought up on opposite sides of a plume conduit. The two-plume model is less likely based on the discussion above.

One implication of the single bilateral plume model for the 1998 Ma Povungnituk-MintoLIP is the southern domain would imply a LLSVP existed at this time. Based on published paleomagnetic data on the Minto dykes (Buchan et al., 1998), the inferred paleo-latitude and orientation of the boundary between LLSVP (southern domain) and ambient mantle (northern domain) at this time are shown in Fig. 13. Note both northern and southern hemisphere options are shown with uncertainty as to which paleomagnetic polarity option applies. Accordingly, this suggests a new technique for locating LLSVPs in the Paleozoic and Precambrian:

1) Search for LIP events that have a bilateral chemistry and characterize their chemistries, and assess which would be comparable to a LLSVP.
2) Use paleomagnetism to determine the paleo-latitude and paleo-orientation of the edge of the LLSVP implied by the LIP bilateral chemistry.
3) Assuming a number of LIPs exhibit such bilateral chemistry, then build up a dataset on the location of LLSVP boundaries and the evolved LLSVP compositions for a variety of plume centre locations, and through time.

Such a dataset could test whether these Paleozoic and Precambrian LLSVPs are consistent with the current pattern of two major LLSVPs (Torsvik et al., 2010, 2014) allowing the testing of models in which new LLSVPs are created during each supercontinent cycle (Li and Zhong, 2009) or whether the two main LLSVPs have been present for at least 300 myr and potentially through much of Earth history (Torsvik et al., 2010, 2014). Supporting persistent ancient mantle heterogeneities (proto-LLSVPs?), Rizo et al. (2016) argued for Hadean reservoirs displaying W isotopic anomalies as a source for modern LIPs (the North Atlantic Igneous Province and the Ontong Java Plateau).

7. Conclusions

A new U—Pb baddeleyite maximum age of 1998 ± 6 Ma has been obtained for a dolerite sill belonging to the mafic Povungnituk Group (MPG) of the Cape Smith Belt and matched to the flood basalts on the basis of geochemistry. This represents the first direct U—Pb age on mafic magmatism of the Povungnituk Group (Beauparlant Fm.). The previously correlated 2038 Ma Korak sills likely belong to a separate LIP event.

The similarity in age among Povungnituk, Watts and Minto units suggests a widespread event in the northern Superior craton covering over 400,000 km^2. The orientation of the Minto dykes would suggest a magmatic center (plume center) in Hudson Bay situated along the extrapolated trend of the Minto swarm which we can intersect with a westward extension of the interpreted rift-related Povungnituk flood basalts.

Distinct geochemical differences can be observed between the northern and southern domains of the Minto-Povungnituk LIP. The northern domain, consisting of the MPG and the Watts Group, is characterized by uncontaminated rocks created by mixing of depleted mantle and an enriched plume component ($\varepsilon_{Nd}^{1998\ Ma} = +4$ and $+1$, respectively). The southern domain, comprising the Minto dykes and the Eskimo Formation basalts, was fed by an even more enriched source ($\varepsilon_{Nd}^{1998\ Ma} = -4$) with the basaltic magmas undergoing additional crustal contamination.

Two different processes can cause this geochemical difference. Plume-induced melting of subcontinental lithospheric mantle beneath the Superior craton could have formed magmas that differ sufficiently in composition and isotopic signature from melts generated by mixing of a plume head and depleted ambient mantle. Another possible cause could be the direct transport of different primary compositions in two adjacent plumes, or within a single plume, from deep mantle sources. In the latter interpretation the different plume compositions would remain on separate sides of the plume during ascent and would imply that the two spatially separated compositions in the Minto-PovungnitukLIP directly represent the composition of the deep mantle on different sides of the plume at the time of emplacement. The alternate interpretation of two nearby but separate coeval plumes would also imply two distinct compositions of the deep mantle. Given this example, bilateral asymmetry in LIP events could then be used as a tool to map and locate deep mantle anomalies (like the modern LLSVP) back through Earth's history.

Acknowledgements

Sm—Nd isotopic work has been assisted by Shuangquan Zhang. This publication represents publication number 65 from the IGGRC. Additional Samples have been provided by M.R. St-Onge. Nico Kastek has

been supported by the 2010–2015 LIPs –Supercontinent Reconstruction – Resource Exploration Project.

R. Ernst has been partially supported from Mega-Grant14. Y26.31.0012 of the Russian Federation. This is publication number 73 of the 2010–2015 LIPs –Supercontinent Reconstruction – Resource Exploration Project (www.supercontinent.org; www.camiro.org/exploration/ongoing-projects).

Appendix A. Supplementary data

Supplementary data to this article can be found online at https://doi.org/10.1016/j.lithos.2018.09.026.

References

Baragar, W.R.A., 2007. Geology, Sleeper Islands, Eastern Hudson Bay, Nunavut. Geological Survey of Canada, Map 2114A, scale 1 : 75 000.
Baragar, W.R.A., 2015. Geology of part of Kovik Bay map area (NTS 35-F). Geological Survey of Canada, Open File 7846, 1.
Baragar, W.R.A., 2017. Geological trans-sections of the Cape Smith Belt in the Nuvilik Lakes map area, Quebec (NTS 35-G); Geological Survey of Canada, Open File 8230, 1.
Baragar, W.R.A., Ernst, R.E., Hulbert, L., Peterson, T., 1996. Longitudinal Petrochemical Variation in the Mackenzie Dyke Swarm, Northwestern Canadian Shield. Journal of Petrology 37, 317–359.
Baragar, W.R.A., Mader, U., Lecheminant, G.M., 2001. Paleoproterozoic carbonatitic ultrabasic volcanic rocks (meimechites?) of Cape Smith Belt, Quebec. Canadian Journal of Earth Sciences 38, 1313–1334.
Bédard, J.H., Harris, L.B., Thurston, P., 2013. The hunting of the snArc. Precambrian Research 229, 20–48.
Blanchard, J.A., Ernst, R.E., Samson, C., 2017. Gravity and magnetic modelling of layered mafic-ultramafic intrusions in large igneous province plume Centre regions: case studies from the 1.27Ga Mackenzie, 1.38Ga Kunene-Kibaran, 0.06Ga Deccan, and 0.13-0.08Ga High Arctic events. Canadian Journal of Earth Sciences 54, 290–310.
Bleeker, W., 2014. The quest for better precision and more accuracy: Revisiting upper intercept ages. Geological Association of Canada Annual Meeting, May 21-23, Fredericton. Abstract 37, 31–32.
Bleeker, W., Ames, D.E., 2017. System-scale and deposit- scale controls on Ni-Cu-PGE mineralisation in cratonic areas and their margins. In: Rogers, N. (Ed.), Targeted Geoscience Initiative, 2016 Report of Activities, pp. 47–53 Geological Survey of Canada, Open File 8199.
Bleeker, W., Ernst, R.E., 2006. Short-lived mantle generated magmatic events and their dyke swarms: The key unlocking Earth's palaeogeographic record back to 2.6 Ga. In: Hanski, E., Mertanen, S., Rämö, T., Vuollo, J. (Eds.), Dyke Swarms – Time Markers of Crustal Evolution, pp. 3–27.
Bleeker, W., Kamo, S.L., 2018. Extent, origin, and deposit-scale controls of the 1883Ma Circum-Superior large igneous province, northern Manitoba, Ontario, Quebec, Nunavut and Labrador. In: Rogers, N. (Ed.), Targeted Geoscience Initiative: 2017 Report of Activities, Volume 2, pp. 5–14 Geological Survey of Canada, Open File 8373.
Boily, M., Leclair, A., Maurice, C., Bédard, J.H., David, J., 2009. Paleo- to Mesoarchean basement recycling and terrane definition in the Northeastern Superior Province, Québec, Canada. Precambrian Research 168, 23–44.
Bryan, S.E., Ernst, R.E., 2008. Revised definition of large Igneous Provinces (LIPs). Earth-Science Reviews 86, 175–220.
Buchan, K.L., Mortensen, J.K., Card, K.D., Percival, J.A., 1998. Paleomagnetism and U–Pb geochronology of diabase dyke swarms of Minto block, Superior Province, Quebec, Canada. Canadian Journal of Earth Sciences 35, 1054–1069.
Buchan, K.L., Goutier, J., Hamilton, M.A., Ernst, R.E., Matthews, W.A., 2007. Paleomagnetism, U-Pb geochronology, and geochemistry of Lac Esprit and other dyke swarms, James Bay area, Quebec, and implications for Paleoproterozoic deformation of the Superior Province. Canadian Journal of Earth Sciences 44, 643–664.
Buchan, K.L., Lecheminant, A.N., van Breemen, O., 2012. Malley diabase dykes of the Slave craton, Canadian Shield: U–Pb age, paleomagnetism, and implications for continental reconstructions in the early Paleoproterozoic. Canadian Journal of Earth Sciences 49, 435–454.
Burgess, S.D., Bowing, S.A., 2015. High-precision geochronology confirms voluminous magmatism before, during and after Earth's most sever extinction. Science Advancements 1.
Campbell, I.H., 1985. The difference between oceanic and continental tholeiites: a fluid dynamic explanation. Contributions to Mineralogy and Petrology 91, 37–43.
Chandler, F.W., 1984. Metallogenesis of an early Proterozoic foreland sequence, eastern Hudson Bay. Canada. Journal of the Geological Society London 141, 299–313.
Chauvel, C., Arndt, N.T., Kielinzcuk, S., Thom, A., 1987. Formation of Canadian 1.9Ga old continental crust. I: Nd isotopic data. Canadian Journal of Earth Science 24, 396–406.
Ciborowski, T.J.R., Minifie, M.J., Kerr, A.C., Ernst, R.E., Bargagar, B., Millar, I.L., 2017. A mantle plume origin for the Palaeoproterozoic Circum-Superior large Igneous Province. Precambrian Research 294, 189–213.
Coffin, M.F., Eldholm, O., 1991. Large igneous provinces. Wiley. United Kingdom, Oxford.
Coffin, M.F., Eldholm, O., 1992. Volcanism and continental break-up; a global compilation of large igneous provinces. Geological Society Special Publications 68, 17–30.
Corrigan, D., 2012. Paleoproterozoic Crustal Evolution and Tectonic Processes: Insights from the LITHOPROBE Program in the Trans-Hudson Orogen, Canada. In: Percival, J.A., Cook, F.A., Clowes, R.M. (Eds.), 40 Tectonic Styles in Canada: The LITHOPROBE Perspective. Vol. 49, pp. 239–286 Geological Survey of Canada, Special Paper.
Devey, C.W., Cox, K.G., 1987. Relationships between crustal contamination and crystallisation in continental flood basalt magmas with special reference to the Deccan Traps of the Western Ghats, India. Earth and Planetary Science Letter 84, 59–68.
Dunphy, J.M., Ludden, J.N., Francis, D., 1995. Geochemistry of mafic magmas from the Ungava orogen, Quebec, Canada, and implications for mantle reservoir compositions at 2.0 Ga. Chemical Geology 120, 361–380.
Ernst, R.E., 2014. Large Igneous Provinces. Cambridge University Press.
Baratoux, L., Söderlund, U., Ernst, R.E., de Roever, E., Jessell, M.W., Kamo, S., Naba, S., Perrouty, S., Metelka, V., Yatte, D., Grenholm, M., Diallo, D.P., Ndiaye, P.M., Dioh, E., Cournède, C., Benoit, M., Baratoux, D., Youbi, N., Bendaoud, A., 2019. New U-Pb baddeleyite ages of dolerite dyke swarms between 1791Ma and 200 Ma, Leo-1 Man Craton, West Africa, and link with the Guiana Shield, South America. In: Srivastava, R.K., Ernst, R.E., Peng, P. (Eds.), Dyke Swarms of the World –A Modern Perspective. Springer (in press).
Ernst, R.E., Bleeker, W., 2010. Large igneous provinces (LIPs), giant dyke swarms, and mantle plumes: significance for breakup events within Canada and adjacent regions from 2.5Ga to the present. Canadian Journal of Earth Sciences 47, 695–739.
Ernst, R.E., Buchan, K.L., 2010. Geochemical Database of Proterozoic Intraplate Mafic Magmatism in Canada. Geological Survey of Canada (Open File 6016).
Ernst, R.E., Jowitt, S.M., 2013. Large Igneous Provinces (LIPs) and metallogeny. In: Colpron, M., Bissig, T., Rusk, B.G., Thompson, J.F.H. (Eds.), Tectonics, Metallogeny, and Discovery: the North American Cordillera and Similar Accretionary Settings, pp. 17–51 Society of Economic Geologists Special Publication 17.
Ernst, R.E., Jowitt, S.M., 2017. Multi-commodity, multi-scale exploration targeting using the Large Igneous Province record. In: Wyche, S., Witt, W.K. (Eds.), TARGET 2017, Perth, Australia: Abstracts. Geological Survey of Western Australia, Record 2017/6, pp. 41–44.
Ernst, R.E., Youbi, N., 2017. How large Igneous Provinces affect global climate, sometimes cause mass extinctions, and represent natural markers in the geological record. Paleogeography, Paleoclimatology, Palaeoecology 478, 30–52.
Ernst, R.E., Bleeker, W., Söderlund, U., Kerr, A.C., 2013. Large Igneous Provinces and supercontinents: toward completing the plate tectonic revolution. Lithos 174, 1–14.
Francis, D.M., Hynes, A.J., 1979. Komatiite-derived tholeiites in the Proterozoic of New Quebec. Earth and Planetary Science Letters 44, 473–481.
Francis, D.M., Hynes, A.J., Ludden, J.N., Bédard, J., 1981. Crystal Fractionation and Partial Melting in the Petrogenesis of a Proterozoic High-MgO volcanic Suite, Ungava, Quebec. Contributions to Mineralogy and Petrology 78, 27–36.
Franics, D., Ludden, J., Hynes, A., 1983. Magma Evolution in a Proterozoic Rifting Environment. Journal of Petrology 24, 556–582.
Gaonac'h, H., Ludden, J.N., Picard, C., Franics, D., 1992. Highly alkaline lavas in a Proterozoic rift zone: Implications for Precambrian mantle metasomatic processes. Geology 20, 24–250.
Halls, H.C., Davis, D., 2004. Paleomagnetic and U–Pb geochronology of the 2.17Ga Biscotasing dyke swarm, Ontario, Canada: evidence for vertical-axis crustal rotation across the Kapuskasing Zone. Canadian Journal of Earth Sciences 41, 255–269.
Hamilton, M.A., Goutier, J., Buchan, K.L., 2016. Minto Large Igneous Province: a 2.00Ga mafic magmatic event in the eastern Superior craton based on U-Pb baddeleyite geochronologyand paleomagnetism. Acta Geologica Sinica (English Edition) Vol. 90, Supp.1 2016 Abstract of the Seventh International Dyke Conference, "Dyke Swarms: Keys to Paleogeographic Reconstruction" August 18–20, 2016, Beijing, China, pp. 69–70.
Harris, L.B., Bédard, J.H., 2014. Crustal evolution and deformation in a non-plate-tectonic Archaean Earth: Comparisons with Venus. In: Dilek, Y., Furnes, H. (Eds.), Evolution of Archean crust and early life. Modern approaches in solid earth sciences Vol. 7, pp. 215–291.
Harrison, L.N., Weis, D., Garcia, M.O., 2017. The link between Hawaiian mantle plume composition, magmatic flux, and deep mantle geodynamics. Earth and Planetary Science Letters 463, 298–309.
Harrison, L.N., Weis, D., 2018. The Size and Emergence of Geochemical Heterogeneities in the Hawaiian Mantle Plume Constrained by Sr-Nd-Hf Isotopic Variation Ober ~47 Million Years. Geochemistry, Geophysics, Geosystems 19 (2018), 2823–2842.
Heaman, L., Peck, D., Toope, T., 2009. Timing and geochemistry of 1.88Ga Molson Igneous events, Manitoba: Insight into the formation of a craton-scale magmatic and metallogenic province. Precambrian Research 172, 143–162.
Hegner, E., Bevier, M.L., 1991. Nd and Pb isotopic constraints on the origin of the Purtuniq ophiolite and early Proterozoic Cape Smith Belt, northern Quebec, Canada. Chemical Geology 91, 357–371.
Hollings, P., Fralick, P., Cousens, B., 2006. Early history of the Midcontinent Rift inferred form geochemistry and sedimentology of the Mesoproterozoic Osler Group, northwestern Ontario. Canadian Journal of Earth Sciences 44, 389–412.
Huppert, H.E., Sparks, R.S.J., 1985. Komatiites I: Eruption and flow. Journal of Petrology 26, 694–725.
Hynes, A., Francis, D.M., 1982. A transect of the early Proterozoic Cape Smith foldbelt, New Quebec. Tectonophysics 88, 23–59.
Jones, T.D., Davies, D.R., Campbell, I.H., Wilson, C.R., Kramer, S.C., 2016. Do mantle plumes preserve the heterogeneous structure of their deep-mantle source? Earth and Planetary Science Letter 434, 10–17.
Kogiso, T., Hirschmann, M.M., 2006. Partial melting experiments of bimineralic eclogite and the role of recycled mafic oceanic crust in the genesis of ocean island basalts. Earth and Planetary Science Letters 249, 188–199.

Kogiso, T., Hirschmann, M.M., Frost, D.J., 2003. High-pressure partial melting of garnet pyroxenite: possible maic lithologies in the source of ocean island basalts. Earth and Planetary Science Letters 216, 603–617.
Kopylova, M.G., Afanasiev, V.P., Bruce, L.F., Thurston, P.C., Ryder, J., 2011. Metaconglomerate preserves evidence for kimberlite, diamondiferous root and medium grade terrane of a pre-2.7Ga Southern Superior protocraton. Earth and Planetary Science Letter 312, 213–225.
Krogh, T.E., 1973a. A low contamination method for hydrothermal decomposition of zircon and extraction of U and Pb for isotopic age determinations. Geochimica et Cosmochimica Acta 37, 485–494.
Krogh, T.E., 1973b. A low-contamination method for hydrothermal decomposition of zircon and extraction of U and Pb for isotopic age determinations. Geochimica et Cosmochimica Acta 37, 485–494.
Lambart, S., Laporte, D., Schiano, P., 2009. An experimental study of pyroxenite partial melts at 1 and 1.5 GPa: Implications for the major-element composition of Mid-Ocean Ridge Basalts. Earth and Planetary Science Letters 288, 335–347.
Legault, F., Francis, D., Hynes, A., Budkewitsch, P., 1994. Proterozoic continental volcanism in the Belcher Islands: implications for the evolution of the Circum Ungava Fold Belt. Canadian Journal of Earth Sciences 31, 1536–1549.
Lightfoot, P.C., Hawkesworth, C.J., 1997. Flood Basalts and Magmatic Ni Cu, and PGE Sulphide Mineralization: Comparative Geochemistry of the Noril'sk (Siberian Traps) and West Greenland Sequences. Geophysical Monograph 100, 357–380.
Lister, C.R.B., 1991. The Upward Migration of Self-Convecting Magma Bodies. In: Peters, T., Nicolas, A., Coleman, R.J. (Eds.), The upward migration of self-convecting magma bodies. Ophiolite genesis and evolution of the oceanic lithosphere Muscat, Oman, pp. 107–123.
Lister, J.R., Kerr, R.C., 1990. Fluid-mechanical models of dyke propagation and magma transport. In: Parker, A.J., Rickwood, P.C., Tucker, D.H. (Eds.), Second International Dyke Conference. A. a. Balkema. Rotterdam-Brookfield, International, Adelaide Australia, pp. 69–80.
Lucas, S.B., St-Onge, M.R., 1992. Terrane accretion in the internal zone of the Ungava orogen, northern Quebec. Part 2: Structural and metamorphic history. Canadian Journal of Earth Sciences 29, 765–782.
Machado, N., David, J., Scott, D.J., Lamothe, D., Philippe, S., Gariéy, C., 1993. U–Pb geochronology of the western Cape Smith Belt, Canada: New insights on the age of initial rifting and arc magmatism. Precambrian Research 63, 211–223.
Maurice, C., David, J., O'Neil, J., Francis, D., 2009. Age and tectonic implications of Paleoproterozoic mafic dyke swarms for the origin of 2.2Ga enriched lithosphere beneath the Ungava Peninsula, Canada. Precambrian Research 174, 118–163.
Minifie, M.J., Kerr, C.K., Ernst, R.E., Hastie, A.R., Ciborowski, T.J.R., Desharnais, G., Millar, I.L., 2013. The northern and southern sections of the western ca. 1880Ma Circum-Superior large Igneous Province, North America: the Pickle Crow dyke connection? Lithos 174, 217–235.
Modeland, S., Francis, D., Hynes, A., 2003. Enriched mantle components in Proterozoic continental flood basalts of the Cape Smith foldbelt, northern Québec. Lithos 71, 1–17.
Mungall, J.E., 2007. Crustal contamination of picritic magmas during transport through dikes: the expo intrusive suite, Cape Smith Fold Belt, New Quebec. Journal of Petrology 48, 1021–1039.
Nicholson, S.W., Shirey, S.B., 1990. Midcontinent rift volcanism in the Lake Superior region: Sr, Nd, and Pb isotopic evidence for a mantle plume origin. Journal of Geophysical Research 95 (10), 851–10 868.
Nilsson, M.K.M., Söderlund, U., Ernst, R.E., Hamilton, M., Scherstén, A., Armitage, P.E.B., 2010. Precise U-Pb baddeleyite ages of mafic dykes and intrusions in southern West Greenland and implications for a possible reconstruction with the Superior craton. Precambrian Research 183, 399–415.
Parrish, R.R., 1989. U-Pb geochronology of the Cape Smith Belt and Sugluk block, northern Quebec. Geoscience Canada 16, 126–130.
Pearce, J.A., 2008. Geochemical fingerprinting of oceanic basalts with applications to ophiolite classification and the search for Archean oceanic crust. Lithos 100, 14–48.
Pearce, J.A., Norry, M.J., 1979. Petrogenetic implications of Ti, Zr, Y, and Nb variations in volcanic rocks. Contributions to Mineralogy and Petrology 69, 33–47.
Petermann, M., Hirschmann, M.M., 2003. Partial melting experiments on a MORB-like pyroxenite between 2 and 3 GPa: Constraints on the presence of pyroxenite in basalt source regions from solidus location and melting rate. Journal of Geophysical Research 108.
Petermann, M., Hirschmann, M.M., Hametner, K., Gunther, D., Schmidt, M.W., 2004. Experimental determination of trace element partitioning between garnet and silica-rich liquid during anhydrous partial melting of a MORB-like eclogite. Geochemistry Geophysics Geosystems 5.
Picard, C., 1989a. Petrologic et volcanologie des roches volcaniques Proterozoiques de la partie centrale de la fosse de 1'Ungava. Ministre de 1'Energie et des Ressources du Quebec, ET87-07.
Picard, C., 1989b. Lithochimie des roches volcaniques ProtCrozoiques de la partie occidentale de la fosse de I'Ungava (region au sud du lac Lanyan). Ministre de 1'Energie et des Ressources du Quebec, ET87-14.
Picard, C., 1995. Synthese petrogeochimique des roches volcaniques proterozoiques de la ceinture orogenique de l'Ungava: evolution geologique des Groupes de Povungnituk, de Chukotat et de Parent. Ministkre de 1'Enkrgie et des Ressources du QuCbec.
Randall, W., 2005. U-Pb Geochronology of the Expo Intrusive Suite, Cape Smith Belt, and the Kyak Bay Intrusion, New Quebec Orogen: Implications for the Tectonic Evolution of the Northeastern Trans-Hudson Orogen. M.Sc. thesis. University of Toronto.
Richard, P., Shimizu, N., Allègre, C.J., 1976. 143Nd/146Nd, a natural tracer: an application to oceanic basalts. Earth and Planetary Science Letters 31, 269–278.
Rizo, H., Walker, R.J., Carlson, R.W., Horan, M.F., Mukhopadhjay, S., Manthos, V., Francis, D., Jackson, M.G., 2016. Preservation of Earth-forming events in the tungsten isotopic composition of modern flood basalts. Science 352, 809–812.
Salters, V.J.M., Stracke, A., 2004. Composition of the depleted mantle. Geochemistry Geophysics Geosystems 5.
Samal, A.K., Srivastava, R.K., Ernst, R.E., Söderlund, U., 2019. Mapping and naming of distinct Neoarchean-Mesoproterozoic mafic dyke swarms of the Indian Shield using Google™ Earth images and ArcGIS™ and their possible association to Large Igneous Provinces: current status and future prospects. In: Srivastava, R.K., Ernst, R.E., Peng, P. (Eds.), Dyke Swarms of the World –A Modern Perspective. Springer (in press).
Sandeman, H.A., Ootes, L., Cousens, B., Kilian, T., 2014. Petrogenesis of Gunbarrel magmatic rocks: Homogeneous continental tholeiites associated with extension and rifting of Neoproterozoic Laurentia. Precambrian Research 252, 166–179.
Schmidt, P.W., 1980. Paleomagnetism of igneous rocks from the Belcher Islands, Northwest Territories, Canada. Canadian Journal of Earth Sciences 17 (7), 807–822.
Schoene, B., Samperton, K.M., Eddy, M.P., Keller, G., Adatte, T., Bowring, S.A., Khadri, S.F.R., Gertsch, B., 2015. U-Pb geochronology of the Deccan Traps and relation to the end-cretaceous mass extinction. Science 374, 182–184.
Schulze, D.J., 1989. Constraints on the abundance of eclogite in the upper mantle. Journal of Geophysical Research 94, 4205–4212.
Schwarz, E.J., Fujiwara, Y., 1981. Paleomagnetism of the Circum-Ungava Fold Belt II: Proterozoic rocks of Richmond Gulf and Manitounuk Islands. In: F.H.a. Campbell, F.H.a. (Eds.). Proterozoic basins in Canada, Geological Survey of Canada, Paper 81-10, 255–267.
Scott, D.J., St-Onge, M.R., Lucas, S.B., Helmstaedt, H., 1991. Geology and chemistry of the early Proterozoic Purtuniq ophiolite, Cape Smith Belt, northern Quebec, Canada. In: Peters, T. (Ed.), Ophiolite Genesis and Evolution of the Oceanic Lithosphere. Kluwer, pp. 817–849.
Scott, D.J., St-Onge, M.R., Lucas, S.B., Helmstaedt, H., 1999. The 2.00Ga Purtuniq ophiolite, Cape Smith Belt, Canada: MORB-like crust intruded by OIB-like magmatism. Ofioliti 24, 199–215.
Shaw, D.M., 1970. Trace element fractionation during anataxis. Geochimica et Cosmochimica Acta 2, 237–243. http://sigeom.mines.gouv.qc.ca.
Sleep, N.H., 1992. Time dependence of mantle plumes: some simple theory. Journal of Geophysical Research 97, 20007–20019.
Sleep, N.H., 1996. Lateral flow of hot plume material ponded at sublithospheric Depths. Journal of Geophysical Research 101, 28.
Sobolev, A.V., Hofmann, A.W., Kuzmin, D.V., Yaxley, G.M., Arndt, N.T., Chung, S.-L., Danyushevsky, L.V., Elliott, T., Frey, F.A., Garcia, M.O., Gurenko, A.A., Kamenetsky, V.S., Kerr, A.C., Krivolutskaya, N.A., Matvienkov, V.V., Nikogosian, I.K., Rocholl, A., Sigurdsson, I.A., Sushchevskaya, N.M., Teklay, M., 2007. The amount of recycled crust in sources of mantle-derived melts. Science 316, 412–417.
Söderlund, U., Johansson, L., 2002. A simple way to extract baddeleyite (ZrO2). Geochemistry Geophysics Geosystems 3.
St-Onge, M.R., Lucas, S.B., Parrish, R.R., 1992. Terrane accretion in the internal zone of the Ungava orogeny, northern Quebec. 1: Tectonostratigraphic assemblages and their tectonic implications. Canadian Journal of Earth Sciences 29, 746–764.
St-Onge, M.R., Henderson, I., Baragar, W.R.A., 2004. Geology, Cape Smith Belt and adjacent domains, Ungava Peninsula, Quebec-Nunavut. Geological survey of Canada. Open File 4930 (scale 1:300 000).
St-Onge, M.R., Searle, M.P., Wodicka, N., 2006. Trans-Hudson orogeny of North America and Himalaya-Karakoram-Tibetan orogeny of Asia: Structural and thermal characteristics of the lower and upper plates. Tectonics 25.
Sun, S.-s., McDonough, W.F., 1989. Chemical and isotopic systematics of oceanic basalts: implications for mantle composition and processes. In: Saunders, A.D., Norry, M.J. (Eds.), Magmatism in the Ocean Basins. Geological Society, London, pp. 313–345.
Torsvik, T.H., Burke, K., Steinberger, B., Webb, S.J., Ashwal, L.D., 2010. Diamonds sampled by plumes from the core–mantle boundary. Nature 466, 352–355.
Torsvik, T.H., van der Voo, R., Doubrovine, P.V., Burke, K., Steinberger, B., Ashwal, L.D., Trønnes, R.G., Webb, S.J., Bull, A.L., 2014. Deep mantle structure as a reference frame for movements in and on the Earth. Proceedings of the National Academy of Sciences of the United States of America 111, 8735–8740.
Wang, K., Plank, T., Walker, J.D., Smith, E.I., 2002. A mantle melting profile across the Basin and Range, SW USA. Journal of Geophysical Research 107, 5–21.
Weis, D., Garcia, M.O., Rhodes, J.M., Jellinek, M., Scoates, J.S., 2011. Role of the deep mantle in generating the compositional asymmetry of the Hawaiian mantle plume. Nature Geoscience 4, 831–838.
White, R.S., McKenzie, D.P., 1995. Mantle plume and continental flood basalts. Journal of Geophysical Research 100, 17543–17585.
Wignall, P.B., 2001. Large igneous provinces and mass extinctions. Earth-Science Reviews 53, 1–33.
Wignall, P.B., 2005. The link between large igneous province eruptions and mass extinctions. Elements 1, 293–297.
Wilson, L., Head, J.W., 2002. Tharsis–radial graben systems as the surface manifestation of plume-related dike intrusion complexes: models and implications. Journal of Geophysical Research 107.
Wodicka, N., St-Onge, M.R., Scott, D.J., Corrigan, D., 2002. Preliminary report on the U–Pb geochronology of the northern margin of the Trans-Hudson Orogen, central Baffin Island, Nunavut. Geological Survey of Canada. Radiogenic age and isotopic studies, Report 15 12 Current Research 2002-F7.
Wüllner, U., Davies, G.F., 1999. Numerical evaluation of mantle plume spacing, size, flow rates, and unsteadiness. Journal of Geophysical Research 104, 7377–7387.